

HANDBOOK OF PHOTOCHEMISTRY

THIRD EDITION

Marco Montalti
Alberto Credi
Luca Prodi
M. Teresa Gandolfi

with introductory sections by Josef Michl and Vincenzo Balzani

 Taylor & Francis
Taylor & Francis Group

HANDBOOK OF PHOTOCHEMISTRY

THIRD EDITION

Marco Montalti
Alberto Credi
Luca Prodi
M. Teresa Gandolfi

with introductory sections by Josef Michl and Vincenzo Balzani



Taylor & Francis

Taylor & Francis Group

Boca Raton London New York

A CRC title, part of the Taylor & Francis imprint, a member of the Taylor & Francis Group, the academic division of T&F Informa plc.

CRC Press
Taylor & Francis Group
6000 Broken Sound Parkway NW, Suite 300
Boca Raton, FL 33487-2742

© 2006 by Taylor & Francis Group, LLC
CRC Press is an imprint of Taylor & Francis Group, an Informa business

No claim to original U.S. Government works
Version Date: 20130926

International Standard Book Number-13: 978-1-4200-1519-5 (eBook - PDF)

This book contains information obtained from authentic and highly regarded sources. Reasonable efforts have been made to publish reliable data and information, but the author and publisher cannot assume responsibility for the validity of all materials or the consequences of their use. The authors and publishers have attempted to trace the copyright holders of all material reproduced in this publication and apologize to copyright holders if permission to publish in this form has not been obtained. If any copyright material has not been acknowledged please write and let us know so we may rectify in any future reprint.

Except as permitted under U.S. Copyright Law, no part of this book may be reprinted, reproduced, transmitted, or utilized in any form by any electronic, mechanical, or other means, now known or hereafter invented, including photocopying, microfilming, and recording, or in any information storage or retrieval system, without written permission from the publishers.

For permission to photocopy or use material electronically from this work, please access www.copyright.com (<http://www.copyright.com/>) or contact the Copyright Clearance Center, Inc. (CCC), 222 Rosewood Drive, Danvers, MA 01923, 978-750-8400. CCC is a not-for-profit organization that provides licenses and registration for a variety of users. For organizations that have been granted a photocopy license by the CCC, a separate system of payment has been arranged.

Trademark Notice: Product or corporate names may be trademarks or registered trademarks, and are used only for identification and explanation without intent to infringe.

Visit the Taylor & Francis Web site at
<http://www.taylorandfrancis.com>

and the CRC Press Web site at
<http://www.crcpress.com>

Foreword

Photochemists are always looking for information of all sorts. There is often an urgent demand for certain information that seemingly should be, but for some reason is not, conveniently available. All of us have a special reference book or two that we treasure that serve as portals to information that we need right away. Maybe it's a book with some good one liners for a speech we have to deliver or a thesaurus with the *mot juste* that we need to convince our colleagues of the beauty of our science in a lecture. Or maybe it's a reference book of prayers that we go to in desperation when experiments are not working. For a photochemist an ideal reference book provides rapid access to that rate constant, that quantum yield, that triplet energy, that fluorescence spectrum, that actinometer, etc. that suddenly is important in making an argument or checking a hypothesis. Where to find such data conveniently and authoritatively and quickly?

The Handbook of Photochemistry has been a very special reference book for photochemists since the first edition appeared in 1973. The collection of data compiled in this edition was judiciously selected and presented in a user friendly manner such that it was easy to find the pertinent information. At that time important photochemical parameters such as excited state energies, rate constants, spectral information were not conveniently gathered. "The Handbook" was a break through in that regard and presented data with a high level of scholarship. The second edition, which appeared in 1993 built on the excellent scholarship of the first edition.

The third edition (2005) follows in the fine tradition of excellent, user-friendly scholarship, with some additional features. The new edition starts Chapter 1, an overview of the photophysics of organic molecules in solution by Josef Michl, followed by Chapter 2, an overview of the photophysics of transition metal complexes by Vincenzo Balzani. These are welcome essays, well worth reading by students and experts alike. Chapter 3 and the following chapter launch into the "meat" of the Handbook, large tables of data with references on the photophysical properties of organic and inorganic molecules.

The photochemical community will certainly be pleased to see the new updated arrival of The Handbook. Faculty should obtain a copy and put within easy reach of their students. When students ask where can I find...just point them to The Handbook. The sooner they become accustomed to using it as an information resource, the better off their research and understanding of photochemistry will be.

Enjoy.

Nicholas J. Turro
Columbia University (NY)

Preface to the third edition

In our everyday research and teaching activity as photochemists, the Handbook of Photochemistry has always been an invaluable reference. Therefore, needless to say, we embarked in the preparation of this revised and expanded edition of the Handbook with the greatest enthusiasm.

In the last thirteen years, since the release of the second edition of this Handbook, photochemical sciences have continued their vigorous expansion, as witnessed by the ever-increasing number of scientific papers dealing with photochemistry. Many spectroscopic and photochemical techniques that used to be prerogative of specialist research groups are now available in a wide range of laboratories. It has also become evident that chemistry as a whole has evolved rapidly. In many instances the traditional fields of chemistry – organic, inorganic, physical, analytical, biological – tend to overlap and merge together, giving rise to disciplines, such as those related to nanosciences. Light-induced processes play, indeed, an important role in these emerging fields of science. In such a context, we felt that times were ripe for a third edition of the Handbook of Photochemistry.

As for the previous editions, the goal of the third one is to provide a quick and simple access to the majority of the chemical and physical data that are crucial to photochemical investigations – from the planning and set up of experiments to the interpretation of the results. For the preparation of this Handbook, we could profit from an excellent starting material, that is, the second edition by S. L. Murov, I. Carmichael and G. L. Hug, published in 1993. We decided to maintain the format of most of the existing tables of data, not only because they were quite well organized, but also because many scientists got used to them during the years. By taking advantage of modern literature databases and related powerful search engines, we updated and expanded such tables with data on hundreds of new compounds. In particular, the section dealing with reduction potential values (Chapter 7), in the light of the importance of electron-transfer processes in photochemistry, was considerably enriched. In preparing the tabular and graphical material, we devoted a great effort to improve the readability and reach a style uniformity throughout the book.

The most relevant new entries of this third edition are indeed the tables gathering together the photophysical (Chapter 5), quenching (Section 6d) and reduction potential (Section 7b) data on metal complexes and organometallic compounds. Moreover, we found appropriate to expand and update, on the basis of our experience, some of the "technical" sections, and specifically light sources and filters (Chapter 11) and chemical actinometry (Chapter 12). We also introduced a section (Chapter 10) which describes the problems that are most frequently encountered in photoluminescence measurements, and illustrates a simple correction method to take into account the related effects. These sections will hopefully provide preliminary information at a glance, but are not intended to replace the many excellent books on photochemical methods and techniques that are available on the market and cited in the references.

Last but not least, the Handbook now features two introductory chapters written by two world leaders in photochemical sciences. Chapter 1, by Josef Michl, deals with the photophysics of organic molecules in solution. Chapter 2, by Vincenzo Balzani, describes the photophysical properties of transition metal complexes. Again, these sections cannot certainly be adopted in substitution of photochemistry textbooks; however, we felt that a concise overview of the most important light-induced processes that take place in organic and inorganic molecules would have been of help for students and for researchers that wish to get closer to the wonderful world of photochemistry.

In the preparation of this edition we benefited from the contribution of many people. First, we are grateful to all the members of our research group in Bologna, not only for fruitful discussions, but also for their friendship and support. We are particularly indebted to Vincenzo Balzani, Luca Moggi, Alberto Juris, Margherita Venturi of the Department of Chemistry of the University of Bologna, and to Roberto Ballardini of the ISOF Institute of CNR in Bologna. Mara Monari, Serena Silvi, Paolo Passaniti and Alberto Di Fabio gave us invaluable help for typing and checking several parts of the manuscript. Special thanks to Josef Michl for his contribution and Nick Turro for his fine foreword, and all the colleagues around the world that kindly sent us reprints and preprints of their papers or just simple, but precious information.

No book, of course, is free of errors and imperfections. We attempted to keep mistakes at a minimum by careful and repeated checks, and we apologize in advance for those that we could not avoid. We sincerely hope that readers will enjoy this new edition and that it will continue to be "The Handbook" of the photochemical community.

Photochemistry has come a long way since the pioneering work of Giacomo Ciamician, to whom our Department is named after. However, the ideas expressed by Ciamician in his visionary speech of 1912, entitled "The photochemistry of the future" are still the most appropriate to conclude this preface. The following sentence, quoted in the first two editions of the Handbook of Photochemistry, is worth repeating:

"On the arid lands there will spring up industrial colonies without smoke and without smokestacks; forests of glass tubes will extend over the plains and glass buildings will rise everywhere; inside of these will take place the photochemical processes that hitherto have been the guarded secret of the plants, but that will have been mastered by human industry which will know how to make them bear even more abundant fruit than nature, for nature is not in a hurry and mankind is."

G. Ciamician, *Science*, **1912**, 36, 385-394.

*Marco Montalti
Alberto Credi
Luca Prodi
Maria Teresa Gandolfi*

Bologna, May 2005

Contents

<i>Foreword</i>	<i>iii</i>
<i>Preface</i>	<i>v</i>
1 Photophysics of Organic Molecules in Solution	1
1a Introduction	2
1b Electronic States	2
1c Radiative Transitions	24
1d Non-Radiative Transitions	37
1e Excited State Kinetics	43
2 Photophysics of Transition Metal Complexes in Solution	49
2a Electronic Structure	50
2b Types of Excited States and Electronic Transitions	60
2c Absorption and Emission Bands	61
2d Jablonski Diagram	71
2e Photochemical Reactivity	72
2f Electrochemical Behavior	76
2g Polynuclear Metal Complexes	78
3 Photophysical Properties of Organic Compounds	83
3a Photophysical Parameters in Solution	83
3b Triplet-State Energies: Ordered	157
3c Flash-Photolysis Parameters	227
3d Low-Temperature Photophysical Parameters	267
3e Absorption and Luminescence Spectra: a Selection	301
4 EPR and ODMR Parameters of the Triplet State	353
5 Photophysical Properties of Transition Metal Complexes	377
5a Photophysical Parameters in Solution	377
5b Absorption and Luminescence Spectra: a Selection	408
6 Rate Constants of Excited-State Quenching	421
6a Diffusion-Controlled Rate Constants	424
6b Singlet-State Quenching of Organic Molecules	425
6c Triplet-State Quenching of Organic Molecules	439
6d Excited-State Quenching of Transition Metal Complexes	476

7 Ionization Energies, Electron Affinities, and Reduction Potentials	493
7a Ionization Energies and Electron Affinities	493
7b Reduction Potentials	503
8 Bond Dissociation Energies	529
8a Bond Dissociation Energies of Single Bonds	530
8b Bond Dissociation Energies of Small Molecules	533
8c Bond Dissociation Energies of Peroxides and Multiple Bonds	533
9 Solvent Properties	535
9a Physical Properties of Solvents	536
9b Ultraviolet Transmission of Solvents	541
9c O ₂ Concentration in Solvents	542
9d Low-Temperature Organic Glasses for Spectroscopy	549
9e Donor Numbers	553
10 Luminescence Spectroscopy Measurements	561
10a Correction of Luminescence Intensity Measurements in Solution	561
10b Fluorescence Quantum Yield Standards	572
10c Phosphorescence Quantum Yield Standards	576
10d Luminescence Lifetime Standards	577
11 Light Sources and Filters	583
11a Spectral Distribution of Photochemical Sources	583
11b Transmission Characteristics of Light Filters and Glasses	595
12 Chemical Actinometry	601
12a Ferrioxalate Actinometer	602
12b Photochromic Actinometers	604
12c Reinecke's Salt Actinometer	609
12d Uranyl Oxalate Actinometer	611
12e Other Actinometers	611
13 Miscellanea	617
13a Spin-Orbit Coupling and Atomic Masses	617
13b Hammett σ Constants	624
13c Fundamental Constants and Conversion Factors	629
<i>Subject Index</i>	635

1

Photophysics of Organic Molecules in Solution

By Josef Michl, Department of Chemistry and Biochemistry, University of Colorado, Boulder, Colorado 80309-0215, U.S.A.

1a Introduction

1b Electronic States

1b-1 Electronic Wave Functions

1b-2 Potential Energy Surfaces

1b-3 Vibrational Wave Functions

1b-4 Potential Energy Surface Shapes

1b-5 Singlet and Triplet States

1b-6 State Labels

1b-7 Jablonski Diagram

1b-8 Adiabatic Processes

1c Radiative Transitions

1c-1 Electromagnetic Radiation

1c-2 Absorption and Emission

1c-3 Transition Dipole Moment and Selection Rules

1c-4 Linear Polarization

1c-5 Circular Polarization

1c-6 Vibrational Fine Structure

1c-7 Vibronic Coupling

1d Non-Radiative Transitions

1d-1 Non-Born-Oppenheimer Terms

1d-2 Internal Conversion

1d-3 Intersystem Crossing

1d-4 Electron Transfer

1d-5 Energy Transfer

1e Excited State Kinetics

1a INTRODUCTION

The following is a short overview of the principles of photophysics. We start by providing a brief survey of electronic excited states in Section 1b. This material can be found in textbooks of quantum chemistry but we have directed it to the specific needs of those wishing to learn the fundamentals of photophysics. We then proceed to the description of radiative (Section 1c) and non-radiative (Section 1d) transitions between electronic states. Strictly speaking, the material of Section 1c belongs to the discipline of electronic spectroscopy at least as much as it belongs to photophysics, but it was felt that it would be useful to outline the basics here instead of referring the reader elsewhere. Section 1e deals with the procedures that are in common use for the analysis of photophysical and photochemical kinetic data.

1b ELECTRONIC STATES

1b-1 Electronic Wave Functions

Because of their substantially smaller mass, electrons have much less inertia than nuclei and under most circumstances are able to adjust their positions and motion nearly instantaneously to any change in nuclear positions. It is therefore almost always acceptable to separate the problem of molecular structure into two parts, and to write the molecular wave function as a product of an electronic part, parametrically dependent on the nuclear geometry, and a nuclear part, different in each electronic state. The electronic wave function carries information about the motion of electrons within the molecule. Because of their light mass, electrons must be treated by quantum mechanics. The nuclear wave function contains information about molecular vibrational motion. Although strictly speaking nuclear motion must also be treated quantum mechanically, at times it is useful to approximate it by classical mechanics. The separation of electronic and nuclear motion is known as the *Born-Oppenheimer approximation*. The translation of a molecule as a whole is treated separately, almost always by classical mechanics, and need not concern us. Free rotation of an isolated molecule needs to be treated by quantum mechanics, but since we deal only with solutions, where it is severely hindered, we will be able to treat it classically if we need to consider it at all.

Electronic wave functions and their energies are found by solving the electronic Schrödinger equation, assuming stationary nuclear positions. In principle, an infinite number of solutions exists for any chosen geometry. Those at lower energies are quantized and their energy differences are on the order of tens of thousands of cm^{-1} . At higher energies, the energy differences decrease to thousands of cm^{-1} and less, and above the ionization potential, a solution exists at any energy. In the continuum regime, one or more electrons are unbound and the

molecule is ionized (oxidized). For molecules with positive electron affinity, it is also possible to add an electron (reduction).

When only non-relativistic electrostatic energy terms are included in the potential energy part of the Hamiltonian operator contained in the Schrödinger equation, the resulting state wave functions are eigenfunctions of the total spin angular momentum operator and can be classified as singlets, triplets, etc., if the molecule contains an even number of electrons, or doublets, quartets, etc., if the number of electrons is odd. In organic molecules, only singlets and triplets are ordinarily of interest. Among the additional small terms normally neglected in the absence of atoms of high atomic number, spin-orbit coupling and electron spin-spin dipolar coupling are the most important, in that they cause the pure spin multiplet states to mix to a small degree. Also the hyperfine interaction term, which describes the coupling of electron and nuclear spin, can play this role. We shall return to these terms in Sections 1b-7, 1c-2, and 1d-3.

Often, we are only interested in the wave function of the lowest energy, which describes the ground electronic state. In ordinary organic molecules, this is the lowest singlet state (S_0). This wave function is the easiest one to solve for, but even it can only be found very approximately for molecules of any complexity. Most simply, the approximate solutions are expressed in the form of a spin symmetry adapted antisymmetrized product of one-electron wave functions, called an electron configuration state function (Fig. 1b-1). The antisymmetrization is needed to satisfy the Pauli principle, and is achieved by arranging the product of one-electron wave functions into a determinant (the Slater determinant). The one-electron wave functions used are referred to as occupied molecular spinorbitals, and those that could have been used, but were not, are known as virtual or unoccupied molecular spinorbitals, whose number is infinite. The best possible choice of molecular spinorbitals, defined as the one that gives the lowest ground-state energy, carries the name *Hartree-Fock* or *self-consistent spinorbitals*. Physically, a wave function approximated by a single configuration describes the motion of electrons in the field of stationary nuclei and the time-averaged field of the electrons.

Molecular spinorbitals are normally written as a product of an electron spin function (α , spin up, or β , spin down) and a space function, referred to as a molecular orbital. In a closed-shell configuration, each occupied molecular orbital is used twice, once with each choice of spin (Fig. 1b-1). Molecular orbital energies are related to reduction-oxidation properties of ground states of molecules. In an approximation developed by Koopmans, the energy of an occupied Hartree-Fock orbital is equal to minus the energy needed to remove an electron from that orbital to infinity (the ionization potential), and the energy of an unoccupied Hartree-Fock orbital is equal to minus the energy gained when an electron is brought from infinity and added to that orbital (electron affinity).

Molecular orbitals are ordinarily approximated as a linear combination of atomic orbitals centered at the atomic nuclei. These atomic orbitals are known as the basis set. Years of experience have revealed the basis set size and type that are

needed to achieve a desired level of accuracy. Orbitals composed primarily from inner shell atomic orbitals are occupied in all low-energy states. Roughly half of the orbitals derived from atomic orbitals of the atomic valence shell are occupied and the other half are empty. Together, these orbitals span the so-called valence space. Rydberg orbitals are high-energy diffuse orbitals best expressed as combinations of atomic orbitals of higher principal quantum numbers.

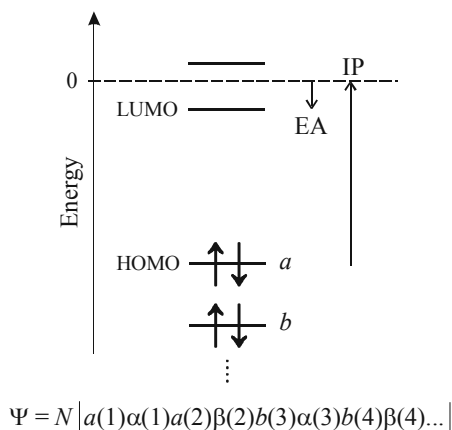


Fig. 1b-1. A symbolic representation of a closed-shell electronic wave function.

It is always better, but especially important at biradicaloid geometries (those with only two electrons in two approximately non-bonding orbitals in low-energy states), not to ignore the instantaneous as opposed to the time-averaged field of the other electrons. The energy lowering associated with this improvement is called electron correlation energy. The most common way to write a correlated wave function is to use a linear combination of many configurations instead of a single one. Depending on the details, this computationally much more demanding procedure is then called configuration interaction, coupled clusters, etc.

It is also possible to avoid molecular orbitals altogether and to construct the molecular electronic wave function directly from hybridized atomic orbitals (linear combinations of atomic orbitals located at the same nucleus). This so-called valence-bond method introduces correlation energy from the outset, but suffers from other difficulties. It has the intuitively appealing feature that the various contributions to the electronic wave function map readily onto the familiar Lewis structures of molecules. Carried to completion within a given starting atomic basis set, the molecular orbital and the valence-bond methods converge to the same result, known as the full configuration interaction wave function. Within the limits dictated by the use of a finite basis set, this is the exact solution of the Schrödinger equation, but present-day computer technology only permits its computation for

very small molecules and limited basis sets, and this is not likely to change in the foreseeable future.

An altogether different approach is to give up the search for the molecular electronic wave function, which is a function of the space and spin coordinates of all electrons present in the molecule and contains far more information than is actually needed for any practical purpose, and to search for the total electron density function instead. Electron density within a molecule only depends on the three spatial variables, and is in principle sufficient for the evaluation of observable quantities. It is evaluated from the so-called Kohn-Sham determinant, built from Kohn-Sham orbitals. Although this determinant is analogous to the Slater determinant of wave function theories, it is not a wave function of the molecule under consideration, but only a construct used to make sure that the search for the optimal density is constrained to those densities for which an antisymmetric wave function in principle exists (it represents a wave function of a fictional molecule whose electrons do not mutually interact, and is chosen so as to produce the best total electron density in the variational sense). The various versions of this so called density functional method differ from each other in the functional used, i.e., in the assumptions they make in evaluating the total energy from electron density distribution in space. This relation is exact in principle and includes contributions from electron correlation energy, but the true form of the requisite functional is not known. The most popular functionals are semiempirical in that their general form agrees with first principles but the details have been adjusted empirically to yield optimal agreement with various experimental results.

Usually, the energy calculation is repeated for many stationary nuclear geometries and the one that yields the minimum total energy for the molecule is referred to as the optimized geometry of the ground state. The single-configuration approximation has the best chance of being adequate at geometries close to this optimized geometry, whereas at biradicaloid geometries the use of one of the methods that include electron correlation is mandatory. At these geometries, density functional methods usually have difficulties.

In photophysics and photochemistry, several of the lowest energy wave functions and their energies are normally needed. With the exception of the wave function of the lowest triplet state, and sometimes also one of the low-energy singlet states, it is only rarely possible to use the single-configuration approximation for excited states, and for accurate results, methods based on linear combinations of configuration state functions are always used. Optimization of geometries in excited states is possible, but again with the exception of the lowest triplet state, much more difficult than in the ground state. In density functional methods, electronic state energy differences are calculated directly from the ground state electron density. In the vicinity of ground state equilibrium geometries, these so called time-dependent density functional methods perform quite well.

The observable properties of a molecule in a particular electronic state, such as its permanent dipole moment, are obtained as the expectation value of the appropriate operator, such as the dipole moment operator \mathbf{M} , over its electronic wave

function, evaluated at the equilibrium geometry. They can change quite dramatically as a function of the electronic state. More properly, the calculation is repeated for many geometries in the vicinity of the equilibrium geometry and averaged over the molecular vibrational wave function, discussed below. Since the variation of molecular properties over a small range of geometries is usually small, this is rarely necessary unless the observable value vanishes by symmetry at equilibrium.

1b-2 Potential Energy Surfaces

The nuclear geometry of a molecule with N nuclei is specified by the values of $3N-6$ internal coordinates, since three of the total of $3N$ degrees of freedom are needed to describe the location of the center of mass and three to describe rotations relative to a laboratory frame. Only the geometry of a diatomic molecule, which is always linear and therefore has only two axes of rotation, is described by $3N-5$ internal coordinates, i.e., by the bond length alone.

A collection of $3N-6$ internal coordinates at a particular geometry represents a point in a $3N-6$ dimensional mathematical space. A surface produced in a $3N-5$ dimensional graph in which the total molecular electronic energy of the ground state is plotted against the geometry is known as the ground state potential energy surface. In spite of its name, the total electronic energy contains not only the kinetic and potential energy of the electrons, but also the potential energy of the nuclei. It is not easy to visualize multidimensional potential energy surfaces, and it is customary, albeit frequently misleading, to show limited portions of a surface in two-dimensional (Fig. 1b-2) or three-dimensional (Fig. 1b-3) cuts through the $3N-5$ dimensional plot.

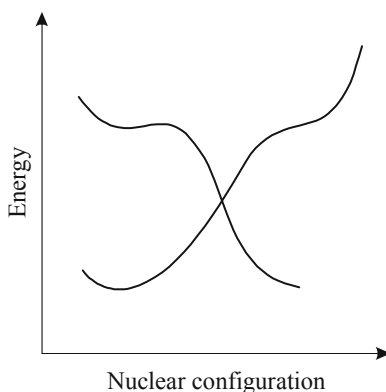


Fig. 1b-2. Two-dimensional cut through potential energy surfaces (schematic).

The ground state potential energy surface contains minima that correspond to the geometries and energies of more or less stable molecules and can be associated with their chemical (Lewis) structures. The minima are separated by barriers, and the lowest cols between minima correspond to transition states of chemical reactions. The height of a col above the minimum is the activation energy, and the width of the col is related to the activation entropy.

Connecting the set of points representing the next higher energy solutions yields the potential energy surface for the first excited state, and one can continue to define potential energy surfaces for as many states as needed (Fig. 1b-2). The excited surfaces also have minima and barriers separating them. Excited state minima located in the geometrical vicinity of a ground state minimum are called spectroscopic since their existence and shape can ordinarily be deduced from molecular electronic spectra. There usually are additional excited state minima and funnels at other geometries, particularly biradicaloid ones. Funnels are conical intersections, $(3N-8)$ -dimensional subspaces in which one potential energy surface touches another, i.e., an electronic state has the same energy as the one just below or just above it. If the two touching states have equal multiplicity, their touching is avoided in the remaining two dimensions. Plotted in these two dimensions, the potential energy surfaces of the two states have the appearance of two conical funnels touching at a single point, the lower upside down and the upper right side up (Fig. 1b-3). Plotted along a single coordinate that passes through a touching point, they look like two crossing lines (Fig. 1b-2). If they have different multiplicity, potential energy surfaces cross freely. The minima and conical intersections in a potential energy surface are often separated by barriers with cols. Minima and funnels located at geometries far from any ground state minima can be referred to as reactive (see below).

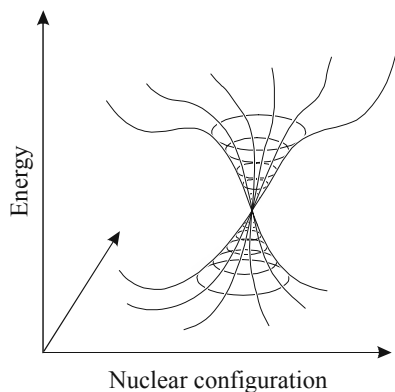


Fig. 1b-3. Three-dimensional cut through potential energy surfaces (perspective view, schematic).

1b-3 Vibrational Wave Functions

The total internal energy of a molecule is obtained by adding the internal nuclear kinetic energy to the electronic energy described by the potential energy surface. At any one time, the molecular geometry is represented by a point in the $3N-6$ dimensional nuclear configuration space, and thus by a point on the potential energy surface. The total energy is represented by a point located vertically above the latter, by an amount corresponding to the nuclear kinetic energy. In a molecule that is not exchanging energy with its environment, the total energy is constant, and the point representing the total energy moves in a horizontal plane, directly above the point that represents the electronic energy, which is located on the potential energy surface (Fig. 1b-4).

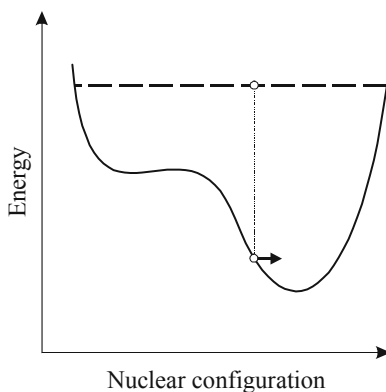


Fig. 1b-4. A schematic representation of the force vector acting on nuclei at a particular choice of nuclear configuration.

In contemplating nuclear dynamics one can invoke an analogy to a balloon soaring at a constant height above a mountainous landscape containing sharp peaks reaching almost to infinity at geometries in which two or more nuclei come very close together. The lateral force acting on the balloon above any one point is given by minus the gradient of the potential energy surface at that point. In completely flat regions of the surface, at its minima, cols, and other points where the gradient of the surface is zero, the force vanishes, and at other points, the force pushes the balloon away from peaks in the general direction of valleys leading toward a nearby minimum. When ground is far below, the balloon moves fast, and when it is close, the balloon slows down.

In the classical limit, and in an appropriately chosen coordinate system, the molecule behaves as if the shadow of the balloon, with the sun at zenith, were to follow the path of a ball that rolls on the surface without friction. In the quantum mechanical description, solutions of the Schrödinger equation for nuclear motion

dictated by the potential energy surface need to be found. The resulting nuclear wave functions have a simple analytic form only in regions where the surface is harmonic, i.e. where a cut through the potential energy surface in any direction is a parabola. This generally occurs in the deep minima located in the vicinity of equilibrium geometries. In each such region, the molecule behaves as a $3N-6$ dimensional harmonic oscillator with frequencies $\nu_1, \nu_2, \dots, \nu_{3N-6}$.

The nuclear eigenfunctions of a $3N-6$ dimensional harmonic oscillator are products of $3N-6$ wave functions, each describing motion along one of the normal modes q_i . Excitation of each of the normal modes is quantized. The stationary energy levels are equally spaced and are labeled by vibrational quantum numbers ν , starting with $\nu = 0$ at the lowest energy. The energy separation is $h\nu$, with the $\nu = 0$ level located at $h\nu/2$ above the minimum of the parabola, at the so called zero point energy. The lowest energy wave function in each mode is Gaussian shaped and the higher energy ones have the form of a Gaussian multiplied by a polynomial. Each has ν nodes. The total vibrational energy is the sum of the vibrational energies in each mode, and the energy in the lowest vibrational state is the sum of zero-point energies in all normal modes (Fig. 1b-5).

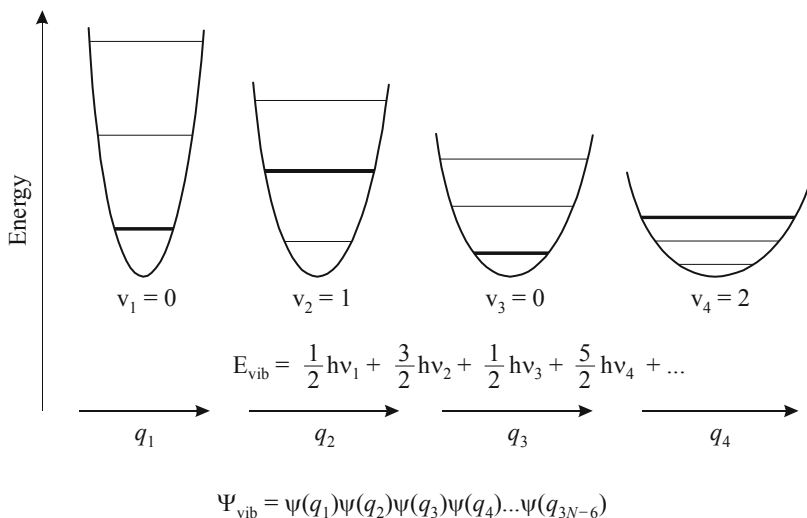


Fig. 1b-5. Contributions of the first few normal modes q_1 – q_4 to vibrational energy (their total number is $3N-6$).

As one departs from the equilibrium geometry, deviations of the potential energy surface from a harmonic shape generally become more pronounced. At higher energies, vibrational wave functions and their spacing therefore deviate increasingly from the simple harmonic behavior. The effects of moderate anhar-

monicity can be treated as a perturbation of the harmonic case, in which the normal modes are only somewhat mixed and the spacing of levels within them is denser. At high nuclear kinetic energies, the normal mode picture breaks down altogether, and it is usually best to view the motion in terms of local modes, oscillators that correspond to individual bonds in the molecule. At the dissociation limit, the total energy is sufficient to break the weakest bond in the molecule. Above this point, the dissociation continuum is reached and vibrational energy is no longer quantized. Accurate quantum mechanical description of nuclear dynamics in highly vibrationally excited molecules is presently only possible in molecules containing very few atoms, and the standard procedure for larger molecules is to calculate a large number of classical trajectories and average the results, or to use statistical theories.

Vibrational eigenfunctions are calculated in the same manner for higher (electronically excited) potential energy surfaces. In regions of local minima, the harmonic approximation is again useful, but the location and shapes of minima are generally different than in the ground potential energy surface. Even in spectroscopic minima, there will be some displacement of the equilibrium geometry, some change in the vibrational frequencies, most often a decrease, and some change in the definition of the normal mode coordinates (which is known as the *Dushinsky effect*).

1b-4 Potential Energy Surface Shapes

An accurate determination of potential energy surfaces, even for small molecules, requires heavy computation, and very few global surfaces are known. After all, even in a tetraatomic molecule, the nuclear configuration space has six dimensions, and even if one wished to have only ten points along each direction, an energy calculation at 10^6 points would be needed. Most often, only very small regions of the space at low energies are explored. Even this is sufficiently demanding that it is often useful to derive qualitative information with minimal or no computations. This provides approximate answers to questions such as “*at which geometries are minima, barriers, and funnels likely to be located?*”, and it also helps with intuitive understanding of the results of numerical computations.

Some general answers are provided by qualitative bonding theory. In the ground state, minima are generally located at geometries that correspond to good Lewis structures, barriers are lower when weaker bonds are being broken and stronger ones made along a reaction path, and they are also lower for orbital symmetry allowed rather than forbidden reactions, etc. Much less chemical intuition is available for electronically excited potential energy surfaces.

Spectroscopic minima are to be expected when electronic excitation does not represent a major perturbation in chemical bonding, particularly in large conjugated systems. Often, they also occur at geometries at which two solute molecules stick to each other in the excited state, even if they do not in the ground state (*excimers* if the two molecules are alike and *exciplexes* if they are different). The

increased intermolecular attraction in the excited state is due to a combination of exciton interactions and charge-transfer interactions in a proportion that depends on the nature of the partners. Since these minima have no ground-state counterpart, they are normally observed spectrally in emission rather than absorption.

Since by definition a spectroscopic minimum in an excited state is located at a geometry not too different from that of the ground state, radiative or radiationless vertical return to the ground state followed by vibrational relaxation typically results in no overall change in molecular structure, and the processes involved are considered a part of photophysics. Yet, spectroscopic minima in the lowest excited singlet and triplet states play an essential role in photochemistry, since they serve as holding reservoirs for excited molecules, with relatively long lifetimes, permitting thermally activated escape over small barriers to reactive minima and funnels located far from ground state geometries. Vertical return from the latter, followed by vibrational relaxation, has the potential to lead ultimately to different ground state species, hence to a photochemical event (Fig. 1b-6).

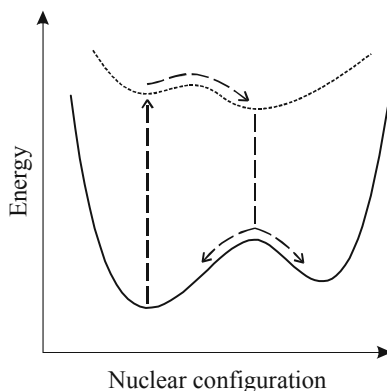


Fig. 1b-6. Motion on potential energy surfaces (schematic).

Reactive minima are to be expected at biradicaloid geometries, those in which the molecule, or a pair of molecules, have one fewer chemical bond than they could have according to the rules of valence. In the ground state biradicaloid geometries are energetically disadvantageous since two electrons in approximately non-bonding orbitals contribute little or nothing to bonding, while at other geometries they could be making a bond. In an excited state, one electron is typically excited from a bonding to an antibonding orbital anyway, more or less cancelling the bonding contribution of its erstwhile partner. There effectively is one bond fewer, and it is no great loss and often actually is an advantage to adopt a biradicaloid geometry and gain two non-bonding electrons. After all, in simple molecu-

lar orbital theory with overlap, an antibonding electron is more antibonding than its bonding partner is bonding, so it is better to have both of them non-bonding.

Exact degeneracy of the two non-bonding orbitals at a perfect biradical geometry leads to a zero energy difference between the lowest and next higher singlet state only in perfect biradicals of the axial type, which are relatively rare (methylnitrene, linear carbene, C_{5h} cyclopentadienyl cation). Ordinarily, and particularly in point biradicals (twisted ethylene, square cyclobutadiene, D_{8h} cyclooctatetraene), there is a considerable separation between S_0 and S_1 . This can be reduced to zero by the introduction of a polarizing perturbation, which removes the exact degeneracy of the two most localized non-bonding orbitals of the biradical (e.g., by distorting square to a diamond cyclobutadiene). Similar recipes for approaching geometries of conical intersections can be formulated using valence-bond theory, and they depend on the similarity of atomic orbital interaction patterns to that observed in the simplest Jahn-Teller case, H_3 .

Perhaps the simplest way to obtain rapid information about likely shapes of potential energy surfaces is to construct a correlation diagram. This tool depends on our ability to plot a sequence of electronic state energies at an initial and a final geometry of a chosen reaction path, or perhaps even at some points in between. These energies can be experimental, calculated, or estimated, but it is essential that an approximate understanding of the nature or at least the symmetry of the corresponding wave functions be available. If one relies on wave function symmetry, only reaction paths preserving that symmetry can be analyzed. However, since potential energy surfaces are continuous, some information about nearby paths is obtained as well.

Lines connecting similar wave functions are then drawn, and the non-crossing rule is invoked. For polyatomic molecules, this rule says that it is rare for two states of equal symmetry to touch (the dimensionality of the subspace of geometries at which touching occurs is only $3N-8$). After the crossings are avoided, a qualitative picture of a cross-section through the potential energy surfaces along the reaction path is obtained and indicates whether barriers or a minima are expected. For instance, if a locally excited and a charge-transfer excited state change their energy order along a reaction path, e.g., in the twisting of *p*-dimethylaminobenzonitrile around its C–N bond from planar to orthogonal geometry, one can expect a barrier in the lower excited surface, and the barrier will be smaller if the two state energies are closer to each other to start with. However, the non-crossing rule does not say how strongly the crossing is avoided, and this needs to be estimated from qualitative arguments or from a calculation. At times, a crossing is avoided so strongly that no trace of it seems to be left in the potential energy surface, and at other times, it is avoided only very weakly, causing the appearance of a barrier in the lower state and a minimum in the upper state. In the latter case, an appropriate reduction of symmetry will often lead from the point of nearest approach to a conical intersection, at which the crossing is not avoided at all, and as noted above, some guidelines are available for such searches. At times, state energies are not available, and then one can start with orbital correlation dia-

grams or valence bond structure correlation diagrams and proceed from these to state correlation diagrams and still obtain useful information.

1b-5 Singlet and Triplet States

A typical singlet wave function of a two-electron system can be written as a product of a function S that depends on the spatial coordinates of the two electrons, and a function that depends on their spin coordinates,

$$\Sigma(1,2) = N[\alpha(1)\beta(2) - \alpha(2)\beta(1)],$$

where $N = 2^{-1/2}$ is the normalization factor. Note that Σ is antisymmetric with respect to the exchange of electrons 1 and 2, so the function of space coordinates S must be symmetric in order for the overall wave function $S\Sigma$ to be antisymmetric and to satisfy the Pauli principle. Typical symmetric spatial functions S could be the closed-shell $a(1)a(2)$ or the open shell $N[a(1)b(2) + a(2)b(1)]$, where the two molecular orbitals a and b are orthogonal.

For a larger even number of electrons, the situation is more complicated in that a larger number of singlet spin functions is possible. For almost all organic molecules, the ground electronic state is a closed shell singlet with all bonding orbitals doubly occupied. Excited singlet states are generally of the open shell kind. The simplest among them can be approximated by a single open-shell configuration, with one unpaired electron in one of the antibonding orbitals and one in one of the bonding orbitals. This wave function can be written as an antisymmetrized product of the open shell wave function written above for two electrons and a closed shell wave function containing all other electrons paired in bonding orbitals. Often, the lowest excited singlet state is of this nature, with the two singly occupied orbitals a and b being the HOMO (highest occupied molecular orbital) and the LUMO (lowest unoccupied molecular orbital) of the molecule. In many aromatic molecules, such as benzene, naphthalene, and their derivatives, this is only the second excited singlet state and an excited singlet state with a more complicated wave function lies lower.

A triplet state consists of a collection of three states (sublevels) that have very similar energies. At room temperature, the populations of the three levels are in rapid equilibrium (equilibration occurs on the scale of ns), but at very low temperatures the equilibrium is established slowly (on the scale of seconds). For the non-relativistic electrostatic Hamiltonian that we have used so far, the three energies are identical. Typical triplet wave functions of a two-electron system can be written as a product of an open-shell function

$$T = N[a(1)b(2) - a(2)b(1)]$$

that depends on the spatial coordinates of the two unpaired electrons located in orbitals a and b and is common to all three sublevels, and one of three functions Θ discussed below that depend on the spin coordinates of the two electrons.

For a larger even number of electrons, the situation is more complicated in that a larger number of triplet spin functions is possible, and they need to be com-

bined to the three functions appropriate for the three sublevels. The simplest among them can again be approximated by a single open-shell configuration, with one electron in one of the antibonding orbitals and the other in one of the bonding orbitals. As was the case for the singlet, this wave function can be written as an antisymmetrized product of the open shell wave function written above for two electrons and a closed shell wave function containing all other electrons paired in bonding orbitals. Almost invariably, the lowest excited triplet state is of this nature, with the two singly occupied orbitals a and b being the HOMO and the LUMO of the molecule.

Simple expressions are available for the energies of excited singlet (1E) and triplet (3E) states of a closed-shell ground state molecule that can be reasonably well described by a single configuration in which an electron has been promoted from an originally doubly occupied orbital a into an originally unoccupied orbital b . Their relation to the orbital energy difference is

$$\begin{aligned}\Delta E &= E(b) - E(a) \\ ^1E &= \Delta E - J_{ab} \\ ^3E &= \Delta E - J_{ab} + 2K_{ab}\end{aligned}$$

where J_{ab} is the Coulomb and K_{ab} the exchange integral between orbitals a and b . The integral J_{ab} can be thought of as the repulsion energy of the charge distribution produced by an electron occupying orbital a with the charge density produced by an electron in orbital b , and typical values are tens of thousands of cm^{-1} . The integral K_{ab} can be thought of as the self-repulsion energy of the overlap charge density (transition density) of orbitals a and b , and typical values are five thousand cm^{-1} or less. The energy of a triplet is therefore approximately $2K_{ab}$ below that of a singlet derived from the same configuration with singly occupied orbitals a and b . K_{ab} tends to be particularly small if the orbitals a and b avoid each other in space, as in charge-transfer or $n\pi^*$ transitions.

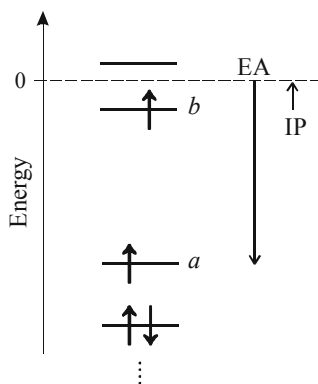


Fig. 1b-7. Electronically excited states have high electron affinities (EA) and low ionization potentials (IP).

Excited molecules are generally much easier to oxidize than ground state molecules, since the singlet or triplet excitation energy counts against the total energy needed to remove an electron to infinity. They are also much easier to reduce, since the excitation energy counts as a net energy gain when the ground state of the radical anion is produced by the addition of an electron. These relations are particularly easy to see for excited states that can be described by single configurations with singly occupied orbitals a and b . The easiest ionization of such an excited state corresponds to the removal of the electron that has been excited to the high-energy orbital b , and its easiest reduction corresponds to the addition of an electron to the low-energy orbital a (Fig. 1b-7).

For all three triplet spin functions the total length of the spin angular momentum vector is $2^{1/2}\hbar$, and the magnitudes of the projection of this vector into the quantization direction are \hbar , 0, and $-\hbar$, with spin quantum numbers 1, 0, and -1 , respectively. Since the three sublevels are degenerate, an arbitrary linear combination can be used, but already a small perturbation that lifts the degeneracy will dictate the quantization direction and the proper choice of spin functions. In the presence of a strong outside magnetic field directed along the laboratory direction Z , as typically applied in EPR spectroscopy, the quantization direction is Z , and the three triplet spin functions are

$$\Theta[1] = \alpha(1)\alpha(2), \quad \Theta[0] = N[\alpha(1)\beta(2) + \alpha(2)\beta(1)], \quad \text{and} \quad \Theta[-1] = \beta(1)\beta(2).$$

The energies of the three sublevels then differ because of the Zeeman term in the molecular Hamiltonian (Fig. 1b-8).

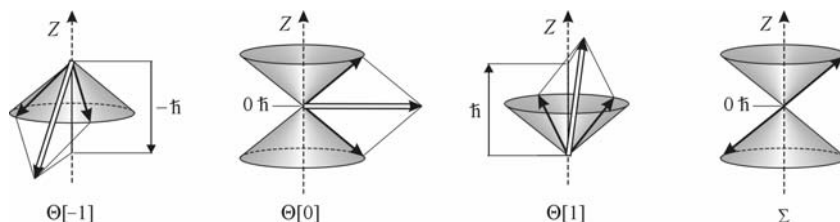


Fig. 1b-8. A symbolic representation of spin angular momenta associated with the triplet (Θ) and singlet (Σ) wave functions in the strong magnetic field limit. Contributions of each of two electrons are shown as simple arrows and their vector sums as double arrows. Projections into the magnetic field direction Z are shown.

If one includes small relativistic terms in the Hamiltonian, the weak interaction of the spin magnetic dipoles of the two unpaired electrons (*spin-spin dipolar coupling*) and the coupling interaction of the magnetic moment due to electron spin with the magnetic moment due to the orbital motion of this and other electrons in the attractive field of nuclei shielded by the other electrons (*spin-orbit coupling*), will cause the energies of the three sublevels to differ a little even in the absence of outside magnetic field. In organic molecules containing no heavy at-

oms, the resulting “zero-field splitting” generally is on the order of one cm^{-1} or less. In the presence of atoms of large atomic number, the effect of spin-orbit coupling can be in hundreds or even thousands of cm^{-1} (the “heavy atom effect”). In atoms and molecules of very high symmetry, such as octahedral or cubic, the effect of the spin dipole-dipole interaction vanishes by symmetry and spin-orbit coupling dominates. In low-symmetry organic molecules containing no atoms of high atomic number, the spin dipole-dipole interaction virtually always dominates the zero-field splitting and the spin-orbit coupling is a minor correction. The energy differences between the three triplet sublevels in the absence of outside magnetic field could be characterized by the energies of the three levels, X , Y , and Z , but it is customary to summarize them in the quantities D and E , defined by

$$D = (X + Y)/2 - Z$$

$$E = (Y - X)/2.$$

They are usually evaluated from EPR spectra.

When spin-orbit coupling is neglected relative to spin-spin dipolar coupling, and there is no outside magnetic field, the orientation of the magnetic axes is given by the principal axes x , y , and z of the spin dipolar tensor, which is fixed in the molecular frame, and the three spin functions are

$$\Theta[x] = N[\alpha(1)\alpha(2) - \beta(1)\beta(2)],$$

$$\Theta[y] = N[\alpha(1)\alpha(2) + \beta(1)\beta(2)],$$

$$\Theta[z] = \Theta[0] = N[\alpha(1)\beta(2) + \alpha(2)\beta(1)].$$

For the function $\Theta[u]$, the projection of the spin angular momentum vector into the axis u is zero ($u = x, y, \text{ or } z$), cf. Fig. 1b-9. When the effects of the outside magnetic field and of the spin-spin dipolar coupling are comparable, the three appropriate spin functions depend on the orientation of the molecule in the field and must be found by matrix diagonalization. Compared to spin-orbit coupling, spin-spin dipolar interaction is ineffective in causing a mixing of electronic states of different multiplicity; for instance, it does not directly mix singlets with triplets.

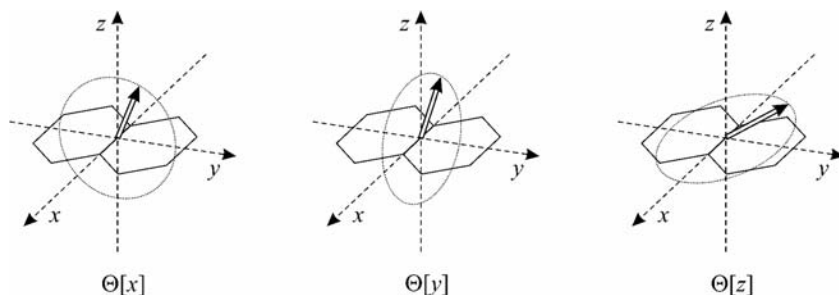


Fig. 1b-9. A symbolic representation of spin angular momenta associated with the triplet (Θ) wave functions in the absence of magnetic field (double arrows). The projection of the angular momentum into the molecular magnetic axis u is zero in the state $\Theta[u]$, $u=x, y, \text{ or } z$.

In organic molecules, the effect of spin-orbit coupling on the first-order description of the triplet sublevels provided above is often described by first order perturbation theory. The totally symmetric spin-orbit operator H^{SO} is approximated as a one-electron operator, and is expressed as a sum of three parts, each of which acts on one of the spin functions $\Theta[u]$ ($u = x, y, z$), which have the symmetry properties of rotation around the axis u . The operator mixes the three triplet sublevels with all singlet and other triplet (and quintet) states I to a degree that is dictated by its matrix elements $\langle I | H_u^{SO} | \Theta[u] \rangle$ and by the energy separation between the states that are being mixed. Although this energy separation is virtually identical for all three sublevels of the triplet, their matrix elements are often vastly different (Fig. 1b-10). Because of the different symmetry properties of the spin functions of the three levels, in symmetric molecules one or more of the matrix elements vanish and different states I are admixed into the wave functions of each sublevel (*spin-orbit coupling selection rules*).

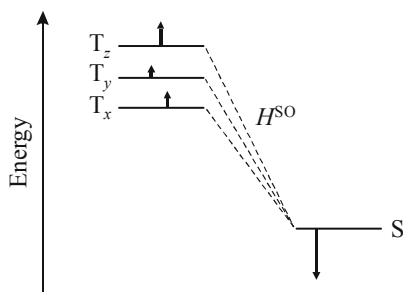


Fig. 1b-10. The arrows show the effect of the spin-orbit coupling operator H^{SO} on the energies of the sublevels of a triplet state and on the energy of a somewhat lower lying singlet state (schematic).

As a result, it is no longer true that the three triplet sublevels share exactly the same spatial part of the wave function T. The introduction of spin-orbit coupling thus has two main effects: it modifies the energies of the three sublevels, changing the zero-field splitting, and it removes the strict separation into states of different spin multiplicities. Each singlet state will contain some triplet character, and each triplet will contain some singlet character. This weak admixture of singlet into triplet states and vice versa plays an essential role in organic photophysics and photochemistry.

1b-6 State Labels

It is frequently necessary to refer to singlet and triplet excited states by name, and several labeling schemes exist. The states are frequently referred to as S_n and T_n , respectively, and numbered in the order of increasing energy, starting with the

lowest singlet state S_0 and the lowest triplet state T_1 . In ordinary organic molecules, S_0 lies below T_1 and represents the ground state, but in rare instances, T_1 lies lower and is the ground state. The same labels can be used for potential energy surfaces, and it is important to adhere to the convention that the states are labeled by the order of their energies; i.e., S_1 cannot be above S_2 at any geometry, by definition. Thus, states with different labels can touch, but they cannot cross, and at points where they touch, they can change their slopes discontinuously (Fig. 1b-11).

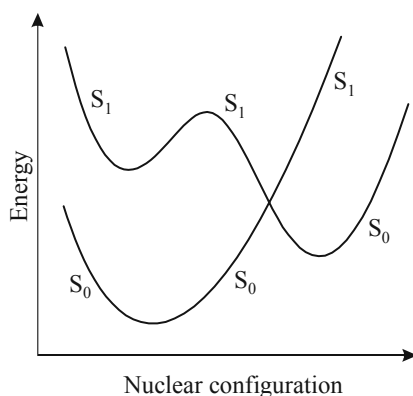


Fig. 1b-11. State labeling convention.

At nuclear geometries with elements of symmetry, such as reflection planes and axes of rotation, it is common to label states by group theory symbols for irreducible representations to which their electronic wave functions belong. In deriving these labels, the symmetry of the triplet spin function is usually not included and the symmetry of the space part of the triplet wave function is used to refer to all three sublevels jointly. The total symmetry for each of the three separate sublevels $\Theta[x]$, $\Theta[y]$, and $\Theta[z]$ is then easily derived by multiplying with the irreducible representations appropriate for rotation about the axes x , y , and z , respectively.

Group theoretical labels are very useful for the derivation of selection rules and in relating similar compounds of a larger family to each other. Although they are strictly applicable only at special points on a potential energy surface, they are often used in a loose sense even in areas near symmetrical geometries, where nuclear symmetry is only approximate.

There are, however, many circumstances in which molecular symmetry is simply too low for any group theoretical classification to be useful. In such cases, the best one can usually do is to provide another indication of the nature of the electronic wave function. A common procedure is to approximate the excited state wave function by a single configuration and to use the symbols of the orbital from

which an electron has been promoted, such as σ , π , or n (lone pair) for the initial orbital and π^* , σ^* , or Rydberg for the terminating orbital of the excitation. The symbols σ and π were originally introduced for linear molecules but it rapidly became common to use them for planar molecules and nowadays they are used in a more general sense to indicate the local symmetry of an orbital, σ for symmetric and π for antisymmetric relative to a local plane of symmetry. The resulting symbols such as $\pi\pi^*$ are useful even for labeling states that cannot be represented by a single configuration, such as the states of benzene, as long as all of the important orbitals out of which promotion took place are of the same class (π) and all of the terminating orbitals are also of the same class (π^*).

Another classification that is often useful is the distinction of locally excited and charge-transfer (CT) states. In the former, the starting and the terminating orbital of the transition are located in the same part of a molecule or pair of molecules, whereas in the latter, they are not. The part of the molecule that carries the starting orbital is referred to as the donor and the part that carries the terminating orbital is called the acceptor.

These types of nomenclature are useful in that they permit the formulation of sweeping statements about electronic transitions. For instance, $n\pi^*$ transitions are never intense, whereas $\pi\pi^*$ transitions can be. While $n\pi^*$ transitions are shifted to higher energies (blue-shifted) in polar and particularly in hydrogen bonding solvents, $\pi\pi^*$ transitions are generally shifted to lower energies (red-shifted). CT transitions are weak, have a small singlet-triplet splitting, and can produce a large change in the state dipole moment.

The labels discussed above are based on molecular orbital description of excited states. An alternative state characterization, based on the valence bond description of its wave function, identifies it as covalent or zwitterionic, depending on the nature of the dominant Lewis structures that symbolize the valence bond wave function. At biradicaloid geometries of uncharged molecules, this designation coincides with the labels “dot-dot” and “hole-pair”, respectively.

1b-7 Jablonski Diagram

A drawing of molecular electronic state energy levels, with singlet and triplet states in separate columns, is referred to as the Jablonski diagram (Fig. 1b-12). Often, vibrational sublevels are shown schematically as well. Radiative transitions from one level to another are indicated by straight arrows and non-radiative ones by wavy arrows. Most often, the levels correspond to vibrationally relaxed electronic states, i.e. to an equilibrium geometry of each individual state. Sometimes, an effort is made to show the state energies at two or more geometries, and as this representation becomes more elaborate, the diagram gradually turns into a drawing of a cut through potential energy surfaces (Fig. 1b-13).

The processes that change the nuclear geometry and/or modify the kinetic energy of the nuclei without changing the electronic potential energy surface that governs the nuclear motions are referred to as *adiabatic*, and are already familiar

from ground state (thermal) chemistry. Those that change the potential energy surface are called *non-adiabatic* (or *diabatic*).

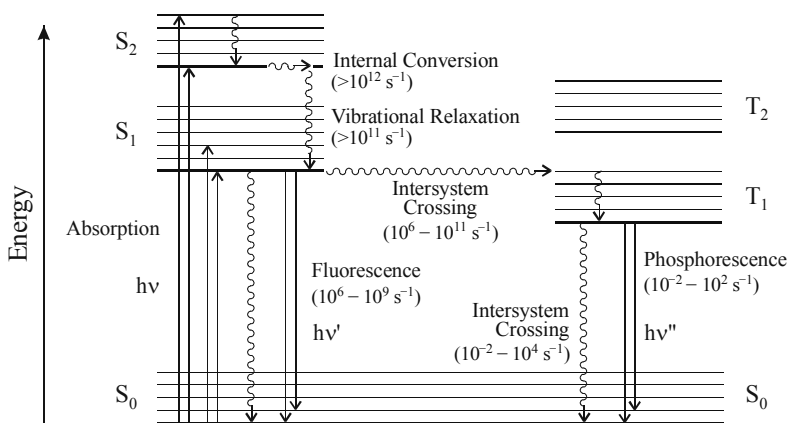


Fig. 1b-12. The Jablonski diagram.

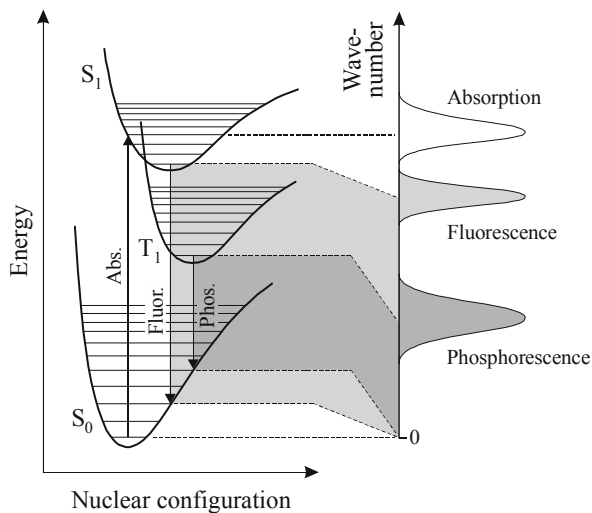


Fig. 1b-13. The relation of observed radiative transitions to potential energy curves (schematic).

1b-8 Adiabatic Processes

Under ordinary circumstances, molecules reside in potential energy minima. At the lowest temperatures, they are in a vibrational ground state. Ordinarily, they are in a state of dynamic equilibrium among all possible vibrational states, described by the Boltzmann distribution, i.e., they are in a thermal vibrational equilibrium. The shape of the potential energy surface in the vicinity of the minimum determines vibrational entropy and heat capacity, and ultimately, along with rotation and translation, the free energy.

In photochemistry and photophysics, we frequently deal with molecules that have vibrational energies much in excess of what would be expected from thermal equilibrium. This may be a result of electronic transition into a higher vibrational level of a state by photon absorption, emission, or energy transfer, or a result of radiationless transition from a higher electronic state. Such molecules remain vibrationally "hot" only for a very short time, since vibrational equilibration in condensed media is very rapid. Even in an isolated molecule, excitation in one normal mode is typically distributed statistically over all internal modes on a ps or sub-ps time scale, and in ordinary solvents, full thermal vibrational equilibrium with the environment is reached in a few ps or tens of ps. In solution, only very fast processes are capable of competing with vibrational equilibration.

In the following, we consider first monomolecular and subsequently bimolecular processes. Occasionally, the degree of vibrational excitation of a molecule exceeds the height of the lowest col in the barriers that surround the minimum (the activation energy). With a probability dictated by the frequency factor, the molecule will find itself going across the col (transition state), escaping into a neighboring minimum or funnel (Fig. 1b-14). The rate of the process is described by transition state theory, in which activation enthalpy and entropy correspond roughly to the energy of activation and the frequency factor, respectively. If the process does not involve the breaking of any chemical bonds, it corresponds to a change in conformation. If the process changes the chemical structure, it corresponds to a chemical reaction.

In the ground electronic state, the distinction between the two possibilities is quite unambiguous. In electronically excited states, it is much harder, and frequently is not made. The main difficulty is that electronic excitation in itself can be viewed as removing one bond, but its antibonding effect is frequently delocalized. To provide a very simple example, there is no doubt that in the ground state a cis and a trans alkene are two different compounds, whose interconversion involves the breaking of a π bond. In the triplet $\pi\pi^*$ state, there again are two minima, both at orthogonally twisted geometries. There is no π bond at any dihedral angle of rotation, and the minima clearly correspond to two conformers of the same molecule. But which bond is missing in the T_1 state of naphthalene? In most instances, the situation is not clear-cut, and we do not even have chemical names for many of the minima in excited state surfaces.

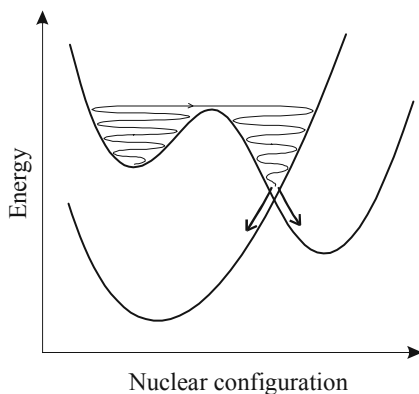


Fig. 1b-14. A symbolic representation of an excited state reaction followed by return to the ground state through a funnel (conical intersection).

Extensive adiabatic nuclear motion in an electronically excited state is quite common in T_1 , and to a much lesser degree, in S_1 . The reason for the difference is that the S_1 state is studded with funnels that can trap a passing molecule and return it to the S_0 state in an extremely rapid diabatic process. In this regard the situation is even less favorable for long-distance adiabatic travel in higher excited states of either multiplicity. Even in T_1 , adiabatic motion typically represents only a fraction of the overall reaction path, since after eventual return to S_0 , a chemical bond can usually be made before the final product geometry is reached.

Other than minor adjustments in internuclear distances and twisting motions, proton translocation is by far the most common type of adiabatic chemical reaction in the S_1 state (Fig. 1b-15), although a few examples of adiabatic C–C bond making and breaking processes have been reported. In organic photochemistry it is exceedingly rare to observe excited singlet product formation, and unusual to observe the formation of a product in its vertically excited triplet state.

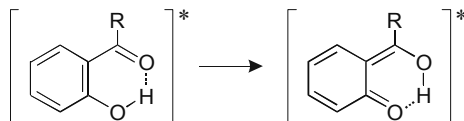


Fig. 1b-15. An example of an adiabatic chemical reaction in the S_1 state.

The description of bimolecular adiabatic processes is similar to the one just given for monomolecular ones. One needs to treat both reaction partners as a “supermolecule” and to include all of their nuclei in constructing the potential energy

surfaces. It is however necessary to recognize that motion along certain directions in the nuclear configuration space is relatively slow. One of the $3N-6$ dimensions corresponds to the intermolecular separation and motion in this direction is limited by the rate of translational diffusion. Five dimensions describe the relative orientation of the two molecules and motion in these directions is limited by the rate of rotational diffusion. The diffusion rates are generally slower than the intramolecular vibrational equilibration that we treated above, and depend strongly on solvent viscosity. In ordinary organic solvents, and at usual reactant concentrations, the typical scale for intermolecular encounters due to these motions is ns.

Under ordinary conditions, the two partners therefore are vibrationally equilibrated before they meet, except in neat or nearly neat liquids. In general, they are attracted to each other by dispersion (van der Waals) forces, and often also by dipole-induced dipole or dipole-dipole forces. At close separation, the dipole approximation to the description of electrostatic interactions is inadequate and the whole charge distribution needs to be considered. Hydrogen bonds are a common source of dimerization and aggregation.

In the gas phase, there is always at least a shallow minimum in the potential energy surface at the geometry of dimer, but in solution the intermolecular force may be purely repulsive if the interaction with the solvent is more favorable than interaction with another solute molecule. Often, however, dimerization or higher aggregation occurs even at relatively low concentrations, especially in poor solvents such as alkanes, and at low temperatures. If one of the partner molecules is an electron donor (reductant) and the other an acceptor (oxidant), intermolecular complex formation is often revealed by the presence of a new electronic transition in the absorption spectrum. This excitation is of charge-transfer character, in that an electron is transferred from the donor to the acceptor. Complexes that exhibit such a transition are called *charge-transfer complexes*, although in their ground state the amount of electron transfer from the donor to the acceptor is usually miniscule (see 1d.4).

As mentioned briefly above, electronically excited molecules are generally even more eager to form dimers and complexes with other molecules. These are referred to as *excimers* (*excited dimers*) and *mixed excimers*, respectively, if they do not exhibit a large degree of charge transfer from one component to the other, and *exciplexes* (*excited complexes*), if they do. Their binding energies are frequently quite significant, comparable to those of hydrogen bonds. When the two partners form a solution charge-transfer complex already in the ground state, these names are not used, and instead, one uses the term *excited charge-transfer complex*.

The formation of excimers and exciplexes occurs on an excited potential energy surface, whether they are formed by an encounter of one excited and one ground state molecule, or, alternatively, by an encounter of a ground state radical anion of one partner with a ground state radical cation of the other (Fig. 1b-16). Although each of the ions is in its electronic ground state, the system of the two ions together is in an electronically highly excited state. Its ground state corre-

spends to a combination of two neutral ground-state molecules and its lowest two excited singlet states usually correspond to combinations of one ground-state and one excited-state neutral molecule, although in certain cases (polar solvents) the ion-pair state can lie below them. In these cases, an adiabatic process connects an exciplex with a pair of ions, whereas normally, an adiabatic process connects it with a pair of neutral molecules, one in its ground and the other in its excited state. Only in rare instances would a pair of dissolved organic molecules have an ionic ground state and be present as a salt.

The only other common case in which intermolecular reactions are adiabatic is proton transfer.

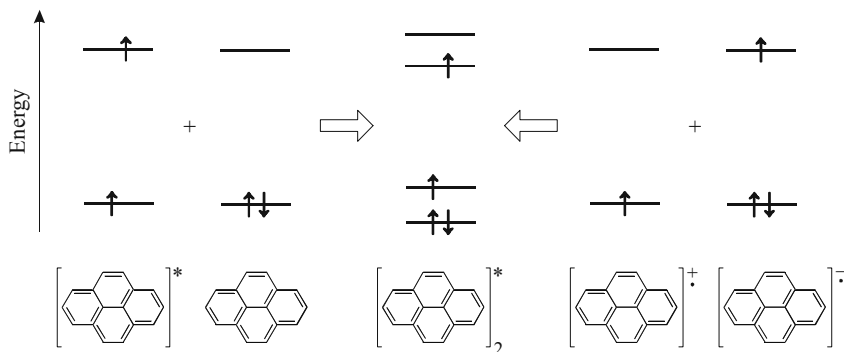


Fig. 1b-16. Generation of pyrene excimer by an encounter of an S_0 with an S_1 excited neutral pyrene molecule (left), and by an encounter of pyrene radical cation with pyrene anion (right).

1c RADIATIVE TRANSITIONS

1c-1 Electromagnetic Radiation

Electronic transitions are most commonly induced by electromagnetic radiation, characterized by its frequency ν and state of polarization, which provides information about the spatial direction of the electric field of the radiation.

The quantum of energy that the radiation field can exchange with matter is $E = h\nu$, which is usually expressed in units of kcal/mol, kJ/mol, or eV/molecule. It is also common to use a quantity proportional to E , such as the frequency ν of the radiation (in s^{-1}), or its wave number $\tilde{\nu} = \nu/c$ (in cm^{-1}). A less useful but also common practice is to use the wavelength of the light, $\lambda = c/\nu$.

Monochromatic light is an abstraction. In practice all light sources produce a distribution of frequencies and wavelengths, and in careful work it is necessary to recognize this and if necessary, integrate over the frequencies present. Lasers produce coherent light, in which the magnitude and spatial direction (polarization) of the electromagnetic wave are well defined at all times. There is a Fourier transform relation between the time dependence of the electric field strength of a pulse of coherent light and the frequency dependence of its spectral distribution, and the shorter is the pulse, the wider is its spectral distribution. Light intensity is proportional to the square of the electric field of the radiation. Other light sources usually produce incoherent light, whose electric field phase is random, but its polarization can still be well defined. For the most common light sources, see Chapter 12.

1c-2 Absorption and Emission

In absorption and emission spectra, light intensity is plotted as a function of one of the characteristics that identify photon energy (Fig. 1c-1). The relation $E = h\nu$ provides a bridge from the position of the observed spectral peaks to the energy difference between initial (G) and final (F) state involved in a spectroscopic transition. The vast majority of transitions are being studied under conditions in which a single photon is absorbed by a molecule at a time, and the *resonant condition* for absorption or emission then is that $h\nu$ be equal to the energy difference of F and G. Simultaneous absorption of two and at times an even larger number of photons is also possible with high laser light intensities. In two-photon absorption, if both photons are taken from the same beam, the resonance condition is that $2h\nu$ be equal to the energy difference of F and G, etc. Some of the advantages of two-photon absorption are a different set of selection rules, higher spatial resolution, and deeper penetration of the longer-wavelength exciting light into otherwise poorly transparent samples, such as biological tissue.

At room temperature equilibrium, organic molecules normally are in their electronic ground state S_0 , and measurement of an absorption spectrum provides information about transitions from S_0 to electronically excited states. It is also possible to transfer a large fraction of molecules to an excited state, typically S_1 or T_1 , usually with an intense laser pulse, and to measure the absorption spectrum of this excited state. Since the excited state population decays rapidly unless continually replenished, this is referred to as *transient absorption spectroscopy*.

Ordinary (one-photon) absorption spectroscopy relies on the *Lambert-Beer law*, which relates the intensity $I(\tilde{\nu})$ of monochromatic light of wave number $\tilde{\nu}$ transmitted through a sample to the intensity $I_0(\tilde{\nu})$ incident on the sample:

$$I = I_0 e^{-\sigma(\tilde{\nu})l} = I_0 10^{-\epsilon(\tilde{\nu})cl}$$

where $\sigma(\tilde{\nu})$ is the absorption coefficient of the sample and l is its thickness. For solutions, it is common to use the molar decadic absorption coefficient (*molar absorptivity*) $\epsilon(\tilde{\nu})$, obtained from the above expression by inserting the molar concentration c and the sample thickness in cm.

In order to observe emission spectra of organic molecules, their excited electronic states first need to be populated. When this is done by light absorption, the emission is referred to as photoluminescence. The measurement can be performed in a continuous mode of excitation (*steady state photoluminescence*) or with pulsed excitation (*pulsed photoluminescence*). Since both the wavelength of the exciting light and that of the detected emitted light can be varied, photoluminescence is intrinsically a two-dimensional spectroscopic technique, but the full two-dimensional spectra are rarely measured. A spectrum showing the dependence on the frequency (or wavelength) of the emitted light is referred to as an *emission spectrum*, and a spectrum showing the dependence on the frequency (or wavelength) of the exciting light of constant intensity is called the *excitation spectrum*. For a correct use of experimental emission and excitation spectra, see Chapter 10.

In the optical region, the wavelength of light is much larger than a molecule, and the electric vector of the radiation E is virtually the same at any point within the molecule. Moreover, the magnetic field carried by the radiation interacts with the molecule much more weakly than the electric field. As a result, the degree of interaction of electromagnetic radiation with the molecule is well described in the electric dipole approximation as $|E \cdot M|^2$, where M is the molecular transition dipole moment of the transition with which the radiation field is resonant, and all magnetic and higher order electric transition moments are neglected. In the absorption event, energy $h\nu$ is transferred from the field to the molecule, and in a stimulated emission event, it is transferred from the molecule to the field. Significant stimulated emission requires relatively intense electromagnetic fields and it is known from laser action. Under most circumstances, *spontaneous photon emission* from an electronically excited state, which takes place even in the absence of radiation imposed from the outside, is more probable. It is induced by the intrinsic zero-field fluctuation of the electromagnetic field that occurs even in vacuum. The rates of the three processes (absorption, stimulated and spontaneous emission) are related by the Einstein relations.

From these relations, Strickler and Berg derived an approximate expression relating the fluorescence rate constant k_F in units of s^{-1} to the integrated intensity of the first absorption band,

$$k_F = (\tilde{\nu}_{\max}^2 / 3.47 \times 10^8) \int (\tilde{\nu}) d\tilde{\nu} \approx \tilde{\nu}_{\max}^2 f 1.5$$

where $\tilde{\nu}_{\max}$ is the wave number of the absorption maximum and f is the oscillator strength, defined by $f = (4.319 \times 10^{-9}) \int \epsilon(\tilde{\nu}) d\tilde{\nu}$.

In the absence of heavy atoms in the molecule, transitions interconnecting S and T states have small transition moments and are referred to as *spin-forbidden*. In absorption, singlet-triplet (and triplet-singlet) transitions have very small extinction coefficients, and are very difficult to observe. Such singlet-triplet absorption spectra consist of three spectrally nearly identical essentially unresolvable contributions, usually of widely different intensities, one into each of the triplet sub-levels. In emission, such transitions have very small radiative constants and very long *natural radiative lifetimes*, and often have low quantum yields since compet-

ing radiationless processes can readily prevail (see Section 1e). The resulting emission is referred to as *phosphorescence*, whereas spin-allowed emission is referred to as *fluorescence* (Fig. 1c-1).

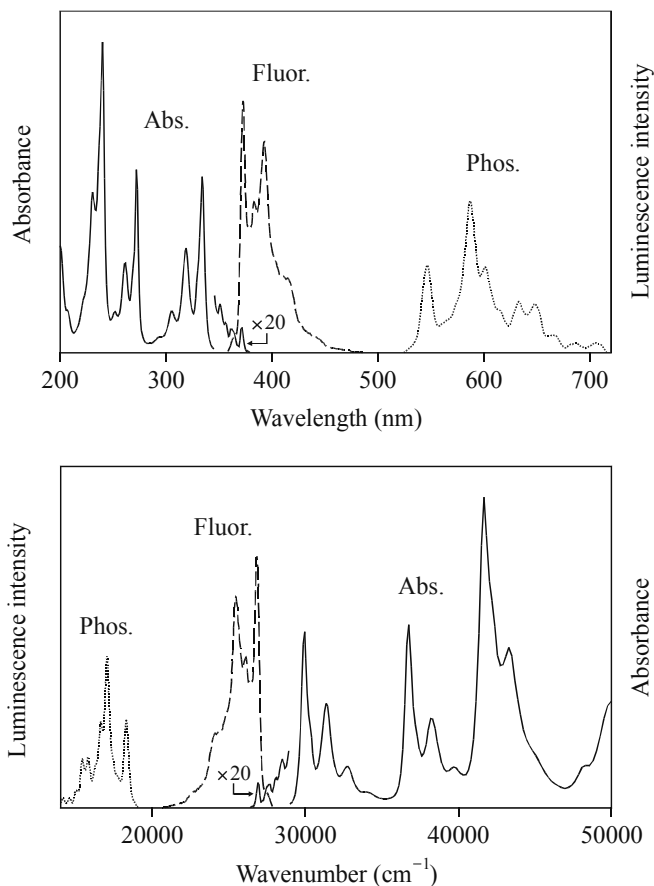


Fig. 1c-1. Absorption and emission spectra of pyrene. Absorption and fluorescence spectra recorded in acetonitrile solution at room temperature; phosphorescence spectrum recorded in acetonitrile rigid matrix at 77 K.

Since the sublevels of a triplet state are typically all populated to some degree, phosphorescence consists of three emissions, one from each sublevel. Their spectral positions ordinarily differ by less than a wave number, much less than the width of the individual peaks in the vibrational structure, and the overlapping emissions cannot be resolved. Commonly, one therefore talks about phosphores-

cence, its polarization degree, quantum yield, etc., as if it were a single emission. The three overlapping emissions can have widely different intensities, even though at equilibrium the three sublevels have nearly exactly the same populations, since one or two of the three emission rate constants are often dominant, especially in symmetrical molecules. One or two of the three competing non-radiative rate constants often dominate as well. Although the triplet excited state is thus drained mostly through one or two of its sublevels, as long as the equilibration of the population among the three levels is rapid, its decay is described by a single exponential, and one refers to a single triplet lifetime. This simplified description of phosphorescence is justified at all but the lowest temperatures.

1c-3 Transition Dipole Moment and Selection Rules

After transition energy, dictated by the difference in the energies of the molecular stationary states involved in the transition, the next most important characteristic of a transition from an initial state G to a final state F is its dipole moment $\mathbf{M}(G \rightarrow F)$. This is a vector whose direction is fixed in the molecular frame but whose sense is not defined (Fig. 1c-2). This is so because it describes the transient electric dipole moment of the transition density, established in the molecule by the perturbing electromagnetic field during the excitation process. During the transition the molecule is not in a stationary state, but in a superposition of the states G and F , and its properties such as the dipole moment oscillate in time. The transition dipole moment \mathbf{M} describes the amplitude and direction of this oscillating electric dipole. It is unrelated to the permanent electric dipole of the molecule in the stationary states G and F , and can be non-zero even in molecules in which the latter vanishes by symmetry. The square of the length of \mathbf{M} is proportional to the integrated transition intensity, and its direction dictates the anisotropy of the transition, in that the transition probability is proportional to $|\mathbf{M}|^2 \cos^2 \alpha$, where α is the angle between \mathbf{M} and the direction of the electric field of electromagnetic radiation (light polarization direction). For a transition moment \mathbf{M} measured in Debye, $f = 4.702 \times 10^{-7} \tilde{\nu} |\mathbf{M}|^2$.

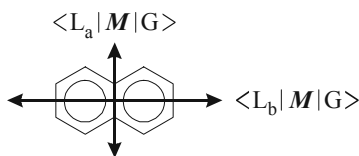


Fig. 1c-2. Transition dipole moments for the excitation of naphthalene from its ground state G to its excited states L_b (S_1) and L_a (S_2).

The quantum mechanical expression for the dipole of the transition electron density is $\langle F | \mathbf{M} | G \rangle$, where $\mathbf{M} = e\mathbf{R}$, e is the (negative) charge of the electron, and

\mathbf{R} is the sum of the position operators of all the electrons in the molecule. None, one, two, or all three components of the transition dipole moment \mathbf{M} may vanish by symmetry, depending on the point group that describes the symmetry of the molecule and on the irreducible representations to which the states G and F belong. Knowledge of state symmetries thus permits a prediction of transition moment directions, referred to as transition polarizations. Conversely, a measurement of transition polarizations is very helpful for the assignment of state symmetries. If all three components of \mathbf{M} vanish, the transition is said to be forbidden by symmetry selection rules, or simply, *symmetry-forbidden*.

If the excitation can be described adequately as the promotion of an electron from orbital a to orbital b , \mathbf{M} is equal to $\langle b | e\mathbf{R} | a \rangle$, where \mathbf{R} now is the position operator of a single electron. This can be thought of as the electric dipole moment of the overlap charge density of orbitals a and b , defined at any point in space by the product of the amplitudes of orbitals a and b at that point (Fig. 1c-3) times electron charge. Overlap charge density is positive in some parts of the molecule and negative in others, and its integral over all space vanishes since it is equal to the overlap of the orthogonal orbitals a and b . Transition moment directions are predictable from the knowledge of orbital symmetries. The general simple rule is that for a transition to be allowed, orbitals a and b should differ by the presence of a single nodal plane, and the polarization direction will be perpendicular to that plane.

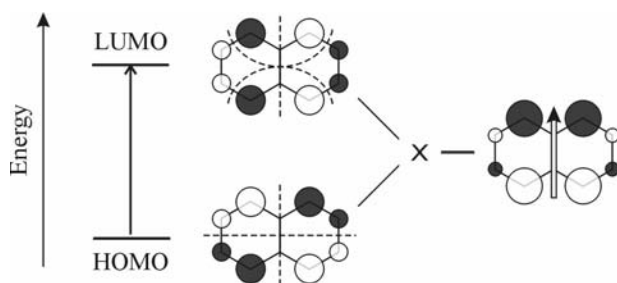


Fig. 1c-3. A schematic representation of the HOMO and LUMO orbitals of naphthalene, and of their product, the transition density for the HOMO \rightarrow LUMO excitation (its dipole moment is indicated with a double arrow).

Even if a transition is allowed, the transition dipole is small if the orbitals a and b avoid each other in space, since then the overlap density is small everywhere and is unlikely to have a large dipole moment. This occurs for instance when a and b are an s and a p orbital on the same atom, as in certain $n\pi^*$ transitions, or when one is mostly distributed over one set of p orbitals in a conjugated system and the other over a separate set, as can happen in non-alternant hydrocarbons (e.g., the first transition in azulene), and in molecules or supermolecules containing an elec-

tron donor with orbital a and an electron acceptor with orbital b separated in space (charge transfer transitions, as in absorption spectra of charge transfer complexes or emission spectra of exciplexes).

The transition moment between states G and F that differ in multiplicity, such as a singlet and a triplet, is generally extremely small in molecules composed of atoms with low atomic numbers. Due to orthogonality of the spin parts of the wave functions G and F, it would actually vanish if the states were not of slightly mixed multiplicity due to spin-orbit coupling. This statement is known as the *spin selection rule*. In molecules with some symmetry, the spin-orbit coupling selection rules mentioned above can be used to deduce the direction of the transition moment into or from each triplet sublevel separately, provided that the symmetries of the spatial parts of the wave functions S and T are known. These directions are normally different for each of the three sublevels.

When an atom of high atomic number Z is introduced into a molecule, spin-orbit coupling almost always increases, often considerably. The resulting increase in singlet-triplet mixing, which is usually quite different for the different sublevels of the triplet, is referred to as the *heavy-atom effect*. Its consequences are an increase in the absorption intensity and in the phosphorescence rate constant. The heavy atom can also be introduced into the solvent rather than the molecule (external as opposed to the internal heavy atom effect). Singlet-triplet mixing can also be induced by the presence of paramagnetic species in the solution, which has similar consequences. For instance, under high pressure of oxygen singlet-triplet absorption of solute molecules becomes quite easily observable.

1c-4 Linear Polarization

If the orientation of an ensemble of absorbing or emitting molecules is random, as is the case in isotropic liquid or solid solutions, light of any polarization is absorbed with equal probability, and emission occurs with equal probability in any direction and with any linear polarization. The former situation is common in absorption spectroscopy of isotropic samples and the latter situation is common in emission spectroscopy of isotropic samples in which excited molecules are equally likely to have any orientation because they were excited randomly, for instance by a chemical reaction (chemiluminescence) or, if they were excited by an anisotropic beam of light, they have had time to rotate into an arbitrary orientation either physically or because of excitation energy transfer (photoluminescence in fluid samples or in concentrated solid samples). The absorption or emission intensity observed on such samples is reduced by a factor of three relative to what would be observed if each molecule were lined up with its transition moment M along the direction of the electric vector of linearly polarized light that is being absorbed or observed in emission.

Fully isotropic measurements of this type provide information about the length of M but not about its orientation in the molecular frame. To obtain the latter, a fully or partially oriented molecular assembly is required. This is most

easily understood by considering measurements on a single molecule and recalling that transition probability is proportional to $|M|^2 \cos^2 \alpha$, where α is the angle between M and the light polarization direction. Except in molecules of very high symmetry neither the initial state G nor the final state F will be degenerate, and at the wave length appropriate for the transition from G to F only a single electronic transition moment M will contribute to the absorption or emission process.

The absorption will be most likely if the light propagation direction is perpendicular to M and the light is linearly polarized parallel to M . Then, α is zero and $\cos \alpha$ has the value of one. A rotation of the light propagation direction by 90° to make it coincide with the direction of M , regardless of its state of polarization, or a rotation of its polarization direction by 90° , which also causes α to become 90° and hence $\cos \alpha$ to vanish, brings the absorption probability to zero. Thus, if the orientation of the molecule is known, a variation of either the light propagation direction or light polarization direction will provide information about the direction of M in the molecular frame. If the direction of M in the molecular frame is known, the measurements will provide information about the orientation of the molecule. The dependence of absorption properties on light direction or polarization is referred to as linear dichroism (LD).

Ordinarily, measurements are performed on molecular assemblies. Fully aligned molecular assemblies occur in crystals and partially aligned ones occur in numerous solutions, liquid (lyotropic or thermotropic liquid crystals, streaming samples, liquids in strong electric or magnetic fields, etc.) or solid (stretched polymers, flat surfaces, etc.). Integration over the orientation distribution function is then necessary to evaluate the results of measurements. The simplest situation prevails in uniaxial samples, which possess a single orientation axis Z , and all directions perpendicular to this axis are equivalent. The choice of the perpendicular axes X and Y is then arbitrary. In this case, only two linearly independent absorption spectra can be obtained and are usually chosen to be those with the light polarization direction either along Z or perpendicular to Z . As in single-molecule measurements, if information about the molecular orientation is available, conclusions about the direction of M in the molecular frame can be reached, and if the latter is known, information about molecular orientation is obtained.

In an entirely analogous fashion, the emission observed from a repeatedly excited oriented molecule through a linear polarizer will be most intense when observed in a direction perpendicular to M with the polarization direction parallel to M . A rotation of the light observation direction by 90° , which makes it coincide with the direction of M , regardless of the rotation of the polarizer, or a rotation of the polarizer by 90° , causes the emission detection probability to vanish. Once again, if the orientation of the molecule is known, a variation of either the light observation direction or polarizer orientation will provide information about the direction of M in the molecular frame. Conversely, if the direction of M in the molecular frame is known, the measurements will provide information about the orientation of the molecule.

Measurements of emission anisotropy or polarization can be performed on the same types of aligned molecular assemblies that were listed above for linear dichroism. Most often, however, it is simplest to produce partially aligned ensembles of excited molecules by photoselection on an isotropic sample in which the molecules are not free to rotate. The best procedure to use for this purpose is to excite the sample with a collimated beam of linearly polarized light. Then, the light electric vector selects molecules for excitation with probabilities given by $\cos^2\alpha$, as we have just seen in the discussion of absorption, and the direction of the light electric field serves as the Z axis of the resulting uniaxial partial oriented assembly. Since the orientation distribution function is then known, specific predictions can be made for the polarization directions to be expected for one or another value of the angle between the absorbing transition moment and the one responsible for the emission. Thus, polarized photoluminescence measurements on rigid solutions, such as organic glasses at low temperatures, produce information about relative polarization directions.

The simplest formulas result if the depopulation of the ground state is negligible and when the observed intensities are cast in the form of emission anisotropy r , defined by

$$r = (I_{\parallel} - I_{\perp}) / (I_{\parallel} + 2I_{\perp})$$

where I_{\parallel} is the emission intensity observed with the analyzing polarizer parallel to the polarization direction of the exciting light, and I_{\perp} is the emission intensity observed with the analyzing polarizer perpendicular to it. Then, if differently polarized transitions do not overlap, $r = 0.4$ if the absorbing and emitting transition moments are parallel, and $r = -0.2$ if they are perpendicular to each other. These limiting values are not always observed in fluorescence measurements, for various reasons. They are less commonly reached in phosphorescence studies, because the differently polarized emissions from three sublevels overlap. Only if emission from one of the sublevels greatly dominates over emission from the other two will there be an opportunity to observe a simple result.

If polarized absorption or emission measurements are performed fast enough after the initial photoexcitation, using short laser pulses and observing the emission at times short relative to rotational diffusion times, similar information can be obtained even in fluid solutions. Moreover, a study of the decay of the polarization anisotropy in time provide information about the rate of molecular rotational diffusion.

1c-5 Circular Polarization

Unlike achiral molecules in an achiral environment, chiral ones, and more weakly, achiral ones in a chiral environment, distinguish left-handed from right-handed circularly polarized light, and absorb and emit the two with slightly different probabilities. This is one of the demonstrations of optical activity. One of two enantiomers has a somewhat larger extinction coefficient ϵ_L for left-handed light, and a somewhat smaller one, ϵ_R , for right-handed light. The mirror image molecule, the

other enantiomer, has the same values of extinction coefficients, but L and R are interchanged. In absorption, the difference spectrum $\epsilon_L - \epsilon_R$ is known as natural circular dichroism (CD). It has positive and negative peaks, and the CD spectra of two enantiomers are mirror images of each other. Racemic samples, which contain equal amounts of the two enantiomers, show a zero CD spectrum, since their contributions cancel.

Each transition from an initial state G to a final state F can be characterized by a rotatory strength $R(G \rightarrow F)$, obtained by integration of the CD spectrum over the transition region. It is positive for one enantiomer and of equal size but negative for the other. Since the CD signal is sometimes easily observable for transitions that are too weak to be seen in absorption because they are covered up by other bands, it can be useful for spectral assignments, and R can be viewed as one of the useful characteristics of an electronic transition. However, the primary practical significance of CD measurements lies elsewhere, as it can be used for the assignment of absolute molecular chirality.

Circular dichroism occurs even in the absence of molecular alignment, and is more complicated and much harder to evaluate for aligned samples. In isotropic solutions, the rotatory strength is related to the scalar product of the electric (\mathbf{M}) and magnetic (\mathbf{M}) dipole transition moment vectors,

$$R(G \rightarrow F) = \text{Im}(\langle G | \mathbf{M} | F \rangle \cdot \langle F | \mathbf{M} | G \rangle)$$

where Im stands for "imaginary part of" and assures a real value for R even though \mathbf{M} is a pure imaginary operator. In molecules that are achiral by symmetry, the two vectors are mutually perpendicular, or one is zero, and the scalar product vanishes. For aligned samples, the expression for rotatory strength is more complicated, and contains a contribution from an electric quadrupole transition moment.

In the presence of magnetic field oriented parallel to the light propagation direction, all samples become optically active and exhibit circular dichroism to a degree proportional to the strength of the magnetic field. This effect is referred to as magnetic circular dichroism, MCD. It is related to the Zeeman effect and has nothing to do with chirality. Unlike natural CD, the MCD spectra of enantiomers are identical and equal to that of a racemic sample. Since MCD changes its sign when the direction of the magnetic field is reversed, the effect disappears when the measuring light is sent through the sample twice in opposite directions, and this permits an easy separation of CD and MCD of chiral samples.

In an MCD spectrum, each transition is characterized by up to three terms, called A , B , and C , normally evaluated by a particular type of integration of the MCD spectrum over the transition region. The first of these vanishes unless the initial or the final state of the transition is degenerate, and the third one vanishes unless the initial state is degenerate. The second one is always present unless the transition has zero intensity in absorption. The B and C terms contribute an identical spectral shape, similar to that of the absorption band, and are separable from each other because C is temperature dependent. The shape contributed by the A term is bisignate and looks like the letter S. The measurement of MCD terms is

useful for spectral assignments, particularly for the recognition of degenerate transitions.

Similar differences between left-handed and right-handed circular polarized light also exist in emission probabilities, where the difference spectra are termed natural and magnetic circular polarized luminescence (CPL and MCPL, respectively). If a transition is somewhat more probable for left-handed circular polarized light in absorption, it is somewhat more probable for right-handed light in emission, and vice versa. CPL is observed for pure enantiomers, even when it is excited with natural or linearly polarized light. It is not observed for achiral molecules in an achiral environment, and only weakly in a chiral environment. It is not observed for racemic mixtures excited with natural or linearly polarized light, but it is observed weakly for racemic mixtures excited with circularly polarized light, since the ensemble of excited molecules is then photoselected to contain slightly more of one of the enantiomers and is no longer racemic. This can be used to distinguish achiral from racemic samples.

1c-6 Vibrational Fine Structure

Electronic transitions in molecules appear as groups of lines. The larger spacings between the individual transitions are due to vibrational structure and reveal the details of vibrational levels in the G and F states. In gas-phase spectra, finer rotational structure also appears. In solutions, only vibrational structure is seen, but its lines are considerably broadened. At low temperatures, and to a lesser degree, even at room temperature, only the lowest vibrational level of the initial state G is significantly populated (all vibrational quantum numbers equal to zero), and this simplifies the consideration of the vibrational fine structure (Fig. 1c-4).

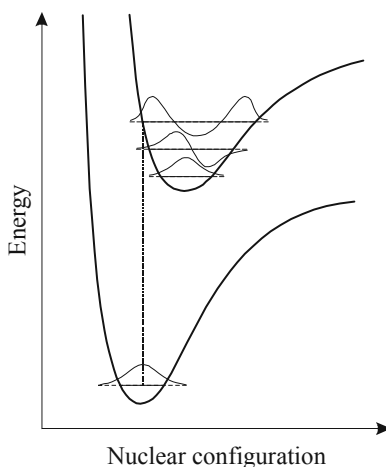


Fig. 1c-4. The origin of Franck-Condon factors (schematic).

Since even the lightest of nuclei are much heavier than electrons, electromagnetic radiation frequencies that are resonant with electronic excitation are much too high to drive an excitation of nuclear motion directly. During electronic excitation, even if it takes a relatively long time (e.g., the time between molecular collisions that destroy wave function coherence), the nuclear vibrational wave function therefore remains nearly intact (*Franck-Condon principle*). If the final electronic state F had a potential energy surface of the same shape as the initial state G (if they had identical vibrational frequencies), and if they were not displaced relative to each other (if they had identical equilibrium geometries), they would share the same set of vibrational wave functions, and only the transitions between levels characterized by identical quantum numbers would appear in the absorption or emission spectra (assuming that the electronic transition moment M is geometry-independent). This situation occurs rarely, since electronic excitation generally causes a modification of bonding conditions in the molecule and thus changes the equilibrium geometry and the force constants. An example is the excitation of inner-shell f electrons in complexes of rare earths.

More commonly, the vibrational wave function i of the initial state I differs from that of the final state F and has a significant non-vanishing projection into those (j) of several or many different vibrational levels of F. Then, transitions into all of the latter levels j will appear in the spectrum at appropriate energies, with probabilities proportional to the so-called Franck-Condon factors, $|\langle j|i\rangle|^2$ if the geometry dependence of M can be neglected. The resulting shape of intensity distribution in the absorption or emission band is often referred to as the Franck-Condon envelope (Fig. 1c-5). The vibrations that appear most prominently in the envelope are those whose normal modes need to be invoked to travel from the equilibrium geometry of the initial state to that of the final state, and those whose frequencies differ the most between the two states. The former are totally symmetric, and all components of the envelope have the same polarization as the zero-zero transition (the band origin). Asymmetric vibrations sometimes appear as double quanta and mark normal modes whose frequency changes strongly between the two states. An analysis of the vibrational fine structure permits a determination of the final state equilibrium geometry if that of the initial state is known. Often, the Franck-Condon envelopes of the absorption and the emission between two electronic states are approximate mirror images of each other in the spectra, since the vibrational frequencies in the two states differ little, and most of the envelope shape is dictated by the displacement of the equilibrium geometry (Fig. 1c-5).

If the change in equilibrium geometry upon excitation is small, the zero-zero transition between the two lowest vibrational levels of the two states is the most intense, and others appear weakly (Franck-Condon allowed transitions). If it is large, the zero-zero transition appears weakly, and sometimes is essentially unobservable (Franck-Condon forbidden transitions). In general, the peak of the absorption or emission band appears approximately at the energy of the so-called vertical transition, which corresponds to the difference between the initial and

final state energy at the equilibrium geometry of the former (Fig. 1c-4). If transitions in both directions can be observed, one in absorption and the other in emission, it is possible to estimate the location of the zero-zero transition as the average of their peak energies, even when the transition itself is too weak to be observed (Fig. 1c-5).

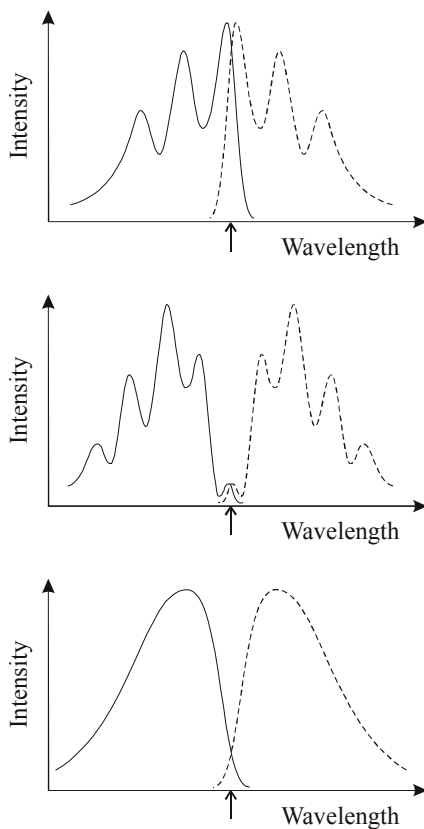


Fig. 1c-5. Examples of Franck-Condon allowed (top) and forbidden (center and bottom) absorption (left) and emission (right). The unresolved spectra shown at the bottom are typical of transitions in which many vibrational modes are active, especially when solvent-solute interactions are strong.

At temperatures at which excited vibrational levels of the initial state are populated, transitions from these levels are observed as well. They are called hot bands and appear at the low-energy side of the transitions from the lowest vibrational level in absorption spectra and at the high-energy side in emission spectra.

In solution spectra, they are often not resolved and merely broaden the spectral bands observed. They are a common cause of thermochromism (dependence of the absorption spectrum on temperature).

1c-7 Vibronic Coupling

The description of the vibrational fine structure given in the preceding section applies to allowed transitions, i.e. those for which at least one of the three components of the transition moment M does not vanish. For transitions that are forbidden, or only very weakly allowed, it is not appropriate to neglect the geometry dependence of M , since in general there will be some symmetry-lowering normal mode that will cause M to differ significantly from zero. Although the origin of the forbidden transition remains forbidden, transitions into levels involving one or a higher odd number of quanta of such asymmetric mode or modes will then appear in the spectrum (*Herzberg-Teller* or *vibronic coupling*), each acting as a "false origin" on which a Franck-Condon envelope of symmetric modes of vibration will be built, using various totally symmetric vibrations. This transition intensity is said to be vibronically induced.

The distortion of the molecular geometry acts as a perturbation that permits mixing of allowed electronic states I that were of different symmetries at the more highly symmetrical equilibrium geometry. This effect introduces some of the non-vanishing transition moments $M(G,I)$ into the otherwise vanishing transition moment $M(G,F)$. Along with this "borrowed" or "stolen" intensity comes its polarization, which is that of the transition from G to I.

In solution, the molecular environment hardly ever has the full molecular symmetry, and it, too, can perturb the symmetry of the molecular wave function away from the one that would otherwise be present. Then, the origin of a forbidden transition will acquire weak but non-zero intensity. E.g., the origin of the lowest singlet-singlet transition in benzene, which is symmetry forbidden and not observed in the gas phase absorption spectrum, is clearly visible in the solution spectrum. The polarization of such solvent-induced transitions is again dictated by the symmetry of the states from which the intensity is borrowed. If the transition from G to F is not forbidden but merely very weak, the direction of its transition moment in solution will be intermediate between $M(G,F)$ and $M(G,I)$. The appearance of these solvent-induced or solvent-enhanced bands is referred to as the *Ham effect*. Their intensity is usually related to the polarizability of the solvent, and they can be used to probe molecular environment.

1d NON-RADIATIVE TRANSITIONS

Transitions between electronic states can occur in a radiationless manner as well as the radiative manner that we have discussed so far (Fig. 1b-12). In both cases, the jump is from a vibrational level of the electronic state associated with one potential energy surface to that of another. In a radiative process, conservation of the

total energy was assured by making up for the acquired energy of electronic motion by absorbing a photon from the radiation field, or making up for the lost energy of electronic motion by donating a photon to the field. In a non-radiative process, conservation of the total energy is assured by compensating for an increase in the energy of electronic motion by taking up energy of nuclear motion, or compensating for the lost energy of electronic motion by releasing it to nuclear motion.

1d-1 Non-Born-Oppenheimer Terms

The coupling between electronic and vibrational motion is mediated by terms in the Hamiltonian that are neglected in the Born-Oppenheimer approximation, and is relatively inefficient. Its rate depends on several factors. The “Franck-Condon factor” drops in size as the number of quanta of vibrational excitation involved grows. This happens with increasing energy difference between the electronic states involved, and upon introduction of heavier isotopes, e.g. in compounds with C-D instead of C-H bonds. The “density of states factor” reflects the number of vibrational levels that are available for the conversion at the energy required. This increases as the energy difference between the electronic states grows, but in general not fast enough to compensate for the fall-off of the Franck-Condon factor. Radiationless transitions thus generally become exponentially slower as the energy difference increases (the *energy gap law*). This can be viewed as paradoxical since it means that a more exothermic process is slower. The “electronic matrix element factor” reflects the difference between the motion that the electrons execute as the molecular geometry changes during vibrational motion. The larger and more abrupt the changes, the harder it is for the electrons to follow the instantaneous changes in the positions of nuclei during vibrations, given that their moment of inertia may be small but is not zero (this is neglected in the Born-Oppenheimer approximation).

Under ordinary circumstances, it is rare for a molecule to have enough vibrational energy to be able to convert it into electronic excitation. It happens in energetic collisions at high temperatures, in intense IR fields, or upon bombardment with energetic particles. In organic molecules, it generally happens only when the energy required for the electronic excitation is fairly small. Thus, in molecules whose T_1 state is only a little below the S_1 state, thermal excitation at room temperature may be sufficient to populate the latter from the former. Because of the generally much longer lifetime of the T_1 state, fluorescence from S_1 can then be observed long after prompt fluorescence from the initially excited S_1 state has decayed (E-type *delayed fluorescence*). Another example is *chemiluminescence*, where thermal excitation from S_0 to S_1 or T_1 takes place in a potential energy surface region where the two are close in energy and is followed by geometry change to a region where S_0 has dropped far down below S_1 or T_1 , such that the excited state produced has a substantial lifetime, and possible vertical emission occurs in the visible region.

Most often, non-radiative transitions convert electronic into vibrational energy, and the latter is lost to the environment within some tens of picoseconds as heat in the process of thermal equilibration. This is the major route of molecular return to the ground state equilibrium after electronic excitation (Fig. 1b-12).

The electronic matrix element that appears in the expression for the rate of a non-radiative process includes an integration over spin that yields unity if the two electronic states are of the same multiplicity. Such spin-allowed non-radiative transitions are known as *internal conversion*. Spin integration causes the matrix element to vanish if the two states involved are of pure spin and differ in multiplicity. The non-radiative transition would then be spin-forbidden. When spin-orbit coupling is included and the two states are of somewhat mixed multiplicity, a non-radiative process known as *intersystem crossing* takes place, but if other factors are the same, it is much slower than internal conversion.

1d-2 Internal Conversion

When the energy difference between the two states between which internal conversion takes place is large and corresponds to the visible or ultraviolet energy region, its rate is often competitive with that of fluorescence. This happens for the S_1 and S_0 states of many colored molecules. The quantum yields of fluorescence and internal conversion are then of comparable order of magnitude. Often, fluorescence dominates strongly when the energy gap is in the ultraviolet or blue whereas internal conversion dominates when the energy gap is in the red, and the lifetimes are on the order of nanoseconds.

When an electronically excited molecule is brought up to another solute, additional dimensions in the nuclear configuration space become accessible and nuclear motion in those directions may lead to internal conversion. Such a process is referred to as excited state quenching, and it can occur at a diffusion limited rate. A common example of a molecule that quenches many excited singlet states is molecular oxygen.

As the energy difference between the two states involved in internal conversion is reduced, its rate increases and the lifetime in the upper state shortens. Since the separations among the higher excited singlets generally are much smaller than the S_1 - S_0 gap, their lifetimes are less than a picosecond with a few exceptions, and fluorescence from higher singlets is not competitive. *Kasha's rule states that only the lowest state of each multiplicity emits, and that all higher excited states convert to it faster than they can do anything else.*

The limit is reached when the potential surfaces of the two states actually or nearly touch (Fig. 1b-3). Then, the rate of internal conversion is normally limited only by the rate at which the molecule can reach this region of the potential energy surface, and this often takes as little as a few tens of femtoseconds. The region of surface touching is known as a conical intersection (see Section 1b-2).

1d-3 Intersystem Crossing

Under otherwise similar circumstances, intersystem crossing is many orders of magnitude slower than internal conversion. The efficiencies of S_1 - S_0 fluorescence are often comparable to those of T_1 - S_0 phosphorescence, reflecting a similar ratio of the rates of radiative and non-radiative processes, but whereas fluorescence lifetimes are typically measured in nanoseconds, those of phosphorescence are often measured in milliseconds or even seconds. This is only true in rigid solution, on surfaces, or in constrained media (cyclodextrins, carcerands, etc.), since in fluid solutions the long lifetimes make phosphorescence superbly sensitive to quenching.

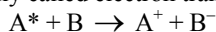
In addition to quenching by impurities and oxygen, triplets also quench each other in a process known as *triplet-triplet annihilation*, in which two triplets encounter and combine their excitation energies to produce an excited singlet and excess vibrational energy. The excited singlet can then fluoresce. Because of the relatively long triplet lifetime, and the continued supply of excited singlets from the annihilation process, the emission continues long after the decay of prompt fluorescence and is known as P-type *delayed fluorescence*. A process inverse to triplet-triplet annihilation is also known and is referred to as *exciton splitting*. It occurs in crystals and polymers and leads to the formation of two triplet excited states from a high vibrational level of an excited singlet state. It is fast enough to compete with vibrational deactivation.

Another illustration of the spin forbiddenness of the intersystem crossing process is the fact that the crossing from S_1 to T_1 is often competitive with the internal conversion from S_1 to S_0 and occurs on a nanosecond time scale, although the energy gap involved is vastly smaller. In this process, the three sublevels of the triplet are generally populated at quite different rates, far from thermal equilibrium. This permits the use of time-resolved EPR spectroscopy to examine the transitions between the sublevels, and can also induce polarization of nuclear spin, permitting the use of CIDNP ("chemically induced dynamic nuclear polarization") for the study of photochemical reactions.

Intersystem crossing is subject to the same kind of internal and external heavy atom effects that have been discussed in connection with phosphorescence (Section 1c-3).

1d-4 Electron Transfer

We have already seen that one of the states participating in a radiative electronic transition can be locally excited while the other is of the charge-transfer type, particularly if the donor and the acceptor are located in different molecules located next to each other. These processes are referred to as charge-transfer absorption (Fig. 1d-1) and charge-transfer (exciplex) fluorescence or phosphorescence. The non-radiative analogs of these charge-transfer processes, internal conversion or intersystem crossing, are usually called electron transfer,



Their rates are subject to similar rules as other non-radiative processes, and have been studied in much detail. They are approximately described by the *Marcus theory*, which also leads to the conclusion that the rates of highly exothermic transfers are low (the “Marcus inverted region”). Because of the spatial separation of the donor and acceptor regions, the splitting between the singlet and triplet states of the dipolar species is particularly small.

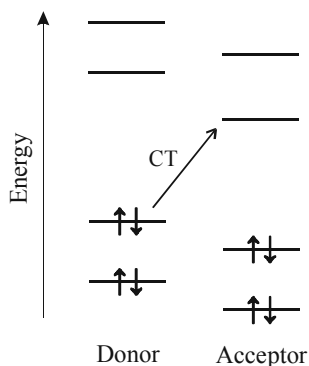
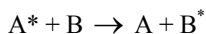


Fig. 1d-1. A schematic representation of a charge transfer transition in absorption.

Electron transfer processes play a crucial role in efforts to convert sunlight to electricity (photovoltaic cells) and to use it for the splitting of water. In both cases, the objective is to separate the generated charges spatially and to prevent their recombination by another non-radiative process to yield the ground state and heat. The charges are then led to electrodes or are used to reduce protons to molecular hydrogen and oxidize hydroxide anions to molecular oxygen.

1d-5 Energy Transfer

Another important class of internal conversion and intersystem crossing processes are of the energy transfer type. In these, both states involved are locally excited, but the excitation is localized in different parts of the molecule or on different molecules,



In addition to the trivial mechanism of energy transfer, in which one molecule emits a photon and another one absorbs it, there are two others (Fig. 1d-2). The *Förster mechanism* operates by an electrostatic coupling of the transition dipole moments of the two partners. It can be visualized as a simultaneous non-radiative deexcitation in the energy donor and excitation in the acceptor. Its rate falls off with the inverse sixth power of their distance, depends on their mutual orientation, and requires energy matching. It is resonant if the two chromophores involved

have the same excitation energy, but normally proceeds downhill, from a chromophore with a higher excitation energy to one with a lower excitation energy. Then, some of the electronic energy is converted into vibrational excitation. Quantitatively, the match is expressed by the overlap of the emission spectrum of the donor and the absorption spectrum of the acceptor. Given the usual fluorescence lifetimes, the Förster mechanism is effective at distances of up to several nm. Since it depends on the transition moments of the partners, and singlet-triplet transition moments are very small, triplet-triplet energy transfer by the Förster mechanism is very slow. This may be compensated by the possibly very long lifetime of the donor triplet state.

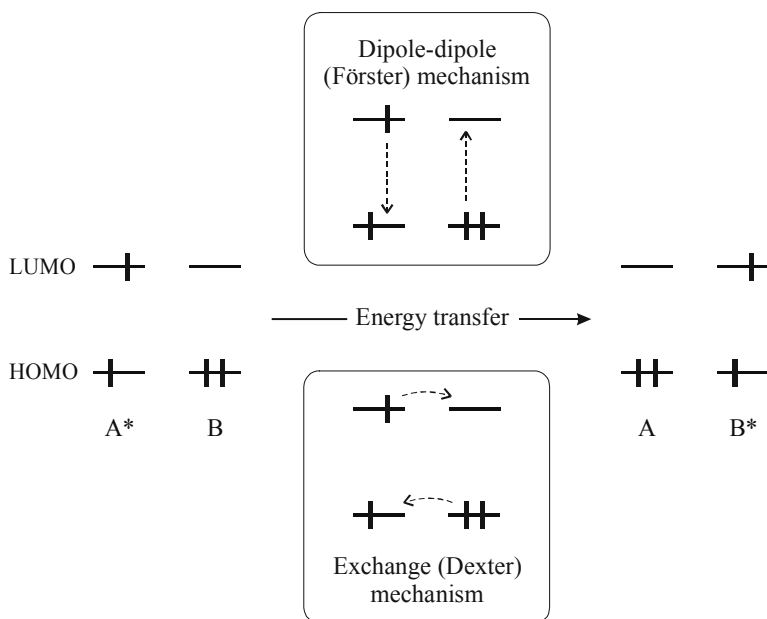


Fig. 1d-2. A schematic representation of the Förster and Dexter mechanisms for energy transfer from A* to B.

The *Dexter* or *exchange mechanism* is short-range and requires interpenetration of the wave functions of the two chromophores. It is best envisaged as a simultaneous transfer of an excited electron from one partner to the other and of its unexcited original counterpart in the opposite direction. As long as the partners effectively touch, it is competitive with the Förster mechanism for singlet excitation energy transfer and vastly faster than the Förster mechanism for triplet excitation energy transfer.

Singlet energy transfer has found much application in structural studies of biomolecules, where it is known under the acronym FRET (Förster resonant energy transfer). Triplet energy transfer has played an essential role in photochemistry, where it is used for excitation of substrates to their triplet state without going through their singlet states (sensitization), and for inducing the return of excited triplet states to the ground state (quenching).

1e EXCITED STATE KINETICS

A complete kinetic analysis of a photophysical or photochemical process requires the determination of the rate constants of all processes that occur, often as a function of their dependence on concentration, solvent, temperature, isotopic labels, and other variables. The basic time-independent observables from which this information is to be deduced are the fluorescence and phosphorescence emission and excitation spectra, quantum yields of fluorescence and phosphorescence of all emitting species, and quantum yields of starting material disappearance and product formation if photochemical transformations occur. The time-dependent observables are the decay curves of all observed emissions and transient absorptions. These basic data are often complemented by the investigation of the effect of quenchers and sensitizers, and sometimes by other measurements, such as photoacoustic calorimetry, CIDNP, etc. In the following, we only provide a brief survey of some of the basics.

The *quantum yield* of a species is measured by determining the number of moles of the species produced upon absorption of a mole of photons (an Einstein). In this sense, a photon of fluorescent or phosphorescent light is considered a species. The efficiency of an elementary step is defined as the fraction of molecules that undergo the step in competition with all other steps possible from the same starting species. The quantum yield of a species is the product of the efficiencies of all the steps that form the path by which it is produced. If a species is formed along more than one path, the contributions of all the participating paths need to be added.

The initial processes that one can anticipate after excitation of an organic molecule with light are formation of one of the excited singlet states and its rapid conversion to the thermally equilibrated lowest excited singlet state on the time scale of a few tens of ps, with a unit efficiency (*Kasha's rule*). Faster processes competitive with this scenario have been observed at times, but they are considered the exception rather than the rule (e.g., direct photochemical reactions that occur by return to the ground state through a conical intersection, or ultrafast intersystem crossing that takes place without prior vibrational equilibration in the S_1 state, especially in the presence of heavy atoms). In general, it is possible to use monochromatic radiation at a wavelength that assures that no state other than S_1 is excited.

The typical processes that compete for the thermally equilibrated S_1 state are fluorescence, internal conversion, intersystem crossing, bimolecular quenching with a quencher Q present at constant concentration [Q], a unimolecular photochemical transformation, and a bimolecular photochemical reaction with a partner B present at a constant concentration [B], with rate constants k_F , k_{IC} , k_{ISC} , $k_Q[Q]$, k_R , and $k_B[B]$, respectively (Figs. 1b-12 and 1d-3).

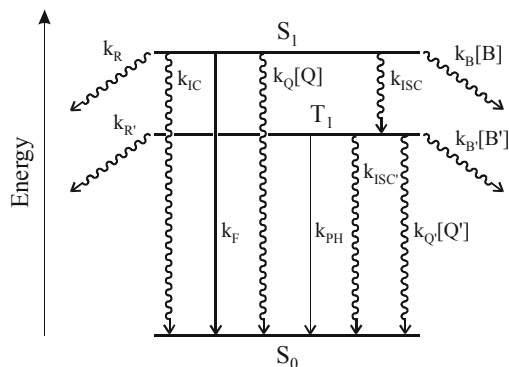


Fig. 1d-3. A list of processes that commonly contribute to a photochemical mechanism.

The *lifetime* of S_1 , i.e. the time needed for its concentration to decay to $1/e$ of its initial value if it is not being replenished, is the inverse of the sum of the unimolecular rate constants of all the processes that depopulate it:

$$\tau(S_1) = 1/(k_F + k_{IC} + k_{ISC} + k_Q[Q] + k_R + k_B[B])$$

The lifetime can be measured by observing the decay of fluorescence intensity after a short pulse excitation, or by monitoring the decay of the transient absorption due to S_1 in time.

The *efficiencies* of the individual steps are

$$\begin{aligned}\eta_F &= k_F \tau(S_1) \\ \eta_{IC} &= k_{IC} \tau(S_1) \\ \eta_{ISC} &= k_{ISC} \tau(S_1) \\ \eta_Q &= k_Q[Q] \tau(S_1) \\ \eta_R &= k_R \tau(S_1) \\ \eta_B &= k_B[B] \tau(S_1)\end{aligned}$$

Assuming that the efficiency with which S_1 is formed is unity, the quantum yield of fluorescence is $\phi_F = \eta_F$. Its measurement thus immediately yields the value of k_F . This can be checked against the value expected from the integrated intensity of the S_1 band in the absorption spectrum (Section 1c-2). The quantum yield of triplet formation is given by $\phi_{ISC} = \eta_{ISC}$ and is harder to determine, unless the transient T_1 absorption spectrum can be measured and the absorption coefficient is known or

can be determined. Then, k_{ISC} can be found. If the product R is only formed from S_1 , its quantum yield is $\phi_R = \eta_R$, and its measurement fixes the value of k_R .

Information on k_Q and k_B can be obtained from a so-called Stern-Volmer plot. For instance, when one measures the fluorescence quantum yield or lifetime for several choices of $[Q]$ and labels them $\phi_F^{[Q]}$ and $\tau(S_1)^{[Q]}$

$$\phi_F^{[Q]} = k_F / (k_F + k_{IC} + k_{ISC} + k_Q[Q] + k_R + k_B[B])$$

$$\tau(S_1)^{[Q]} = 1 / (k_F + k_{IC} + k_{ISC} + k_Q[Q] + k_R + k_B[B])$$

and uses the symbols ϕ_F^0 and $\tau(S_1)^0$ for the values measured in the absence of quencher, one obtains

$$\phi_F^0 / \phi_F^{[Q]} = \tau(S_1)^0 / \tau(S_1)^{[Q]} = 1 + \tau(S_1)^0 k_Q [Q]$$

Thus, when $\phi_F^0 / \phi_F^{[Q]}$ or $\tau(S_1)^0 / \tau(S_1)^{[Q]}$ is plotted against $[Q]$, one obtains a straight line of slope $\tau(S_1)^0 k_Q$ and intercept 1. If $\tau(S_1)^0$ is known, k_Q can be determined, and vice versa. Similar results are obtained when ϕ_F or $\tau(S_1)$ is measured as a function of $[B]$. Often, the quenching can be assumed to be diffusion limited and its rate constant k_Q is of the order $10^{10} \text{ L mol}^{-1} \text{ s}^{-1}$. When the Stern-Volmer plot is curved, the mechanism is more complicated. E.g., two excited states may be involved and only one of them is quenched, or static quenching in pre-formed complexes of the substrate with the quencher intervenes in addition to the dynamic quenching considered so far.

In general, with enough effort, all the rate constants of processes that start in S_1 can be obtained.

The molecules that reach T_1 can again branch. Some will proceed to S_0 by phosphorescent emission with a rate constant k_{PH} , others by intersystem crossing with a rate constant k_{ISC} , some will be quenched with a rate constant $k_Q[Q']$, some will react unimolecularly with a rate constant $k_{R'}$, and some bimolecularly with a rate constant $k_B[B']$. The magnitudes of these rate constants will be obtained in similar ways. For the lifetime of phosphorescence we obtain

$$\tau(T_1) = 1 / (k_{PH} + k_{ISC} + k_Q[Q'] + k_{R'} + k_B[B'])$$

For the efficiency of phosphorescence, we obtain

$$\eta_{PH} = k_{PH} \tau(T_1)$$

and for its quantum yield,

$$\phi_{PH} = \eta_{ISC} \eta_{PH} = k_{ISC} \tau(S_1) k_{PH} \tau(T_1)$$

etc.

Acknowledgments

Support from the US National Science Foundation is gratefully acknowledged. The author thanks Prof. Alberto Credi for preparing the illustrations for this Chapter.

REFERENCES

Theoretical and computational aspects of photophysics

- Michl, J. *Top. Curr. Chem.* **1974**, *46*, 1-59.
- Bonacic-Koutecký, V.; Koutecký, J.; Michl, J. *Angew. Chem. Int. Ed. Engl.* **1987**, *26*, 170-190.
- Michl, J.; Bonacic-Koutecký, V. *Electronic Aspects of Organic Photochemistry*; Wiley: New York (USA), 1990, 475p.
- Domcke, W.; Yarkony, D. R.; Köppel, H. (eds.) *Conical Intersections: Electronic Structure, Dynamics, and Spectroscopy*; World Scientific: Singapore, 2004, 856p.
- Kutateladze, A. G. (ed.) *Computational Methods in Photochemistry*; Marcel Dekker/CRC Press: Boca Raton (FL, USA), volume 13 in the series "Molecular and Supramolecular Photochemistry", 2005, 448p.
- Olivucci, M. (ed.) *Computational Photochemistry*; Elsevier: Amsterdam (The Netherlands), part of the series "Theoretical and Computational Chemistry", 2005, 362p.

Experimental aspects of photophysics

- Birks, J. B. *Photophysics of Aromatic Molecules*; Wiley-Interscience: New York (USA), 1970, 704p.
- Murov, S. L.; Carmichael, I.; Gordon, L. H. *Handbook of Photochemistry*; Marcel Dekker: New York (USA), 1973, 420p.
- Birks, J. B. *Organic Molecular Photophysics*; Wiley and Sons: New York (USA), volume 1, 1973, 600p.; volume 2, 1975, 653p.
- Creation and Detection of the Excited State*; Marcel Dekker: New York (USA), Lamola, A. A. (ed.), volume 1, 1971, parts A and B, 658p.; Ware, W. R. (ed.), volume 2, 1974, 230p., volume 3, 1974, 193p., volume 4, 1976, 320p.
- Lim, E. C. (ed.) *Excited States*; Academic Press: New York (USA) volume 1, 1974, 347p.; volume 2, 1975, 403p.; volume 3, 1977, 351p.; volume 4, 1979, 400p.; volume 5, 1982, 204p.; volume 6, 1982, 224p.
- Burgess, C.; Knowles, A. (eds.) *Standards in Absorption Spectrometry*; Chapman and Hall: London (UK), 1981, 141p.
- Miller, J. N. (ed.) *Standards in Fluorescence Spectrometry*; Chapman and Hall: London (UK), 1981, 112p.
- Rabek, J. F. *Experimental Methods in Photochemistry and Photophysics*; Wiley-Interscience: New York (USA), 1982, part 1, 592p., part 2, 506p.
- Scaiano, J.-C. (ed.) *CRC Handbook of Organic Photochemistry*; CRC Press: Boca Raton (FL, USA), 1989, volume 1, 451p., volume 2, 481p.
- Rabek, J. F. (ed.) *Photochemistry and Photophysics*; CRC Press: Boca Raton (FL, USA), 1991, volume 3, 202p., volume 4, 320p.
- Turro, N. J. *Modern Molecular Photochemistry*; University Science Books: Mill Valley (CA, USA), 1991, 628p.
- Gilbert, A.; Baggott, J. *Essentials of Molecular Photochemistry*; CRC Press: Boca Raton (FL, USA), 1991, 538p.
- Perkampus, H.-H. *UV-VIS Spectroscopy and Its Applications*; Springer-Verlag: Berlin (Germany), 1992, 244p.

- Klessinger, M.; Michl, J. *Excited States and Photochemistry of Organic Molecules*; VCH: New York (USA), 1995, 544p.
- Michl, J.; Thulstrup, E. W. *Spectroscopy with Polarized Light. Solute Alignment by Photoselection*, in *Liquid Crystals, Polymers, and Membranes*; Revised soft-cover edition; VCH: Deerfield Beach (FL, USA), 1995, 573p.
- Lakowitz, J. R. *Principles of Fluorescence Spectroscopy, 2nd Ed.*; Kluwer/Plenum: New York (USA), 1999, 698p.
- Waluk, J. (ed.) *Conformational Analysis of Molecules in Excited States*; Wiley-VCH: New York (USA), 2000, 376p.

2

Photophysics of Transition Metal Complexes in Solution

By Vincenzo Balzani, Department of Chemistry "G. Ciamician", University of Bologna, Italy

2a Electronic Structure

- 2a-1 Crystal Field Theory
- 2a-2 Ligand Field Theory
- 2a-3 Molecular Orbital Theory

2b Types of Excited States and Electronic Transitions

2c Absorption and Emission Bands

- 2c-1 Ligand-Field Bands
- 2c-2 Charge-Transfer Bands
- 2c-3 Intra-Ligand Bands
- 2c-4 A Remark
- 2c-5 Band width

2d Jablonski Diagram

2e Photochemical Reactivity

- 2e-1 Ligand-Field Excited States
- 2e-2 Charge-Transfer Excited States
- 2e-3 Intra-Ligand Excited States
- 2e-4 Remarks

2f Electrochemical Behavior

- 2f-1 Ligand Dissociation Processes
- 2f-2 Structural Changes
- 2f-3 Reversible Processes

2g Polynuclear Metal Complexes

- 2g-1 Supramolecular Species or Large Molecules?
- 2g-2 Electronic Interaction and Intervalence-Transfer Transitions

Transition metal complexes [9901, 0301], which are the most common coordination compounds, may be cationic, anionic or non-ionic species, depending on the charges carried by the central metal atom and the coordinated groups. These groups are usually called *ligands*. Ligands may be attached to the central atom through one or more atoms, i.e. they may be *mono-* or *poly-dentate*. The total number of attachments to the central atom is called *coordination number*. Coordination numbers of 2 to 10 are known, but most coordination compounds exhibit a coordination number of 6 or 4. A given metal ion does not necessarily have only one characteristic coordination number and, moreover, a given coordination number may give rise to several types of spatial arrangements. For example, Ni(II) forms both octahedral six-coordinated and tetrahedral or square-planar four-coordinated complexes. Coordination compounds that contain ligands of two or more types are called *mixed-ligand* complexes.

Many types of isomerism are encountered among transition metal complexes. The most common ones are *geometrical* and *optical isomerisms*. Another important type of isomerism is the *linkage isomerism* which occurs with ligands capable of coordinating in more than one way (ambidentate ligands). For example, the group NO_2^- may coordinate through the nitrogen or the oxygen atom giving rise to *nitro* isomers, such as $[(\text{NH}_3)_5\text{Co-NO}_2]^{2+}$ and to *nitrito* isomers, such as $[(\text{NH}_3)_5\text{Co-ONO}]^{2+}$.

Most of the transition metal complexes are electrically charged species (complex ions) and therefore, they are fairly soluble only in water or other polar solvents. Complex ions, like other charged particles, are particularly sensitive to their environment, i.e. to the nature of the solvent molecules and to the presence of other ionic species. For high ion concentrations, specific effects arise, such as the formation of "ion-pairs" (or "outer-sphere" complexes).

2a ELECTRONIC STRUCTURE

The most correct and complete approach to the electronic structure of metal complexes is that provided by the molecular orbital theory (MOT). Unfortunately, this theory requires a great deal of computation effort in order to provide quantitative results. Consequently, other less meaningful but more handy theories are often used in describing the bonding in complexes. These theories are the crystal field theory (CFT) and the ligand field theory (LFT). The valence bond theory, in its usual form, does not take into account the existence of electronic excited states and thus, it cannot offer any explanation for the photophysical and photochemical behavior.

2a-1 Crystal Field Theory

In this theory [6101, 9501] the ligands are treated as negative point charges which set up an electrostatic field. The effect of this field on the central metal ion is then investigated. Since in the transition-metal ions all but the outermost partially occupied d orbitals are either filled or completely empty, interesting effects, other than those dealt with in the classical ionic theory, arise only from the interaction of the electrostatic field of the ligands with the d electrons.

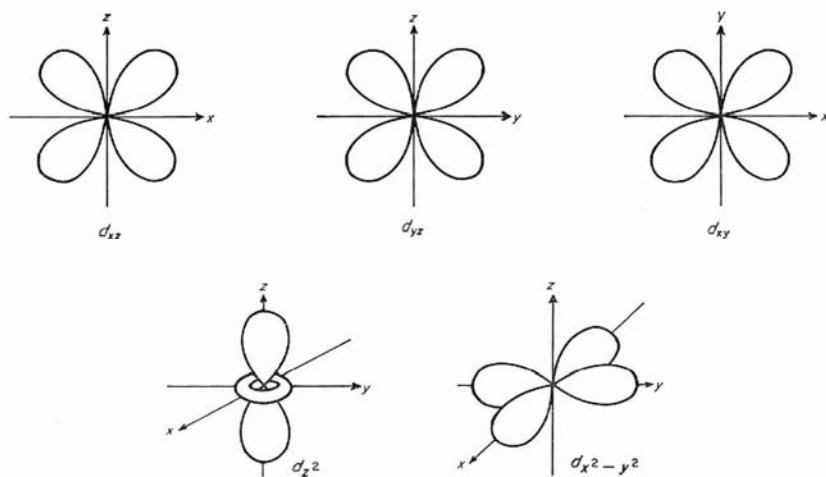


Fig. 2a-1. Pictures of the five d orbitals.

In a gaseous transition-metal ion, the five d orbitals (whose shapes are shown in Fig. 2a-1) are degenerate. In a complex where the ligand field is spherically symmetric, the five d orbitals would be higher in energy than in the free ion, because of the repulsion between the metal ion electron density and the spherical field of negative charge. In such a hypothetical environment, the d orbitals would be still five-fold degenerate. In an actual complex, however, a spherical field is never obtained. Therefore, the five d orbitals, because of their different orientation, are no longer equivalent and they are split according to the particular symmetry of the complex. For example, in a six-coordinated complex having the ligands located on the corners of a regular octahedron, simple pictorial arguments (or better, group-theoretical methods) show that the five d orbitals split into two sets: one set of three orbitals, d_{xy} , d_{xz} and d_{yz} , equivalent to one another and labeled t_{2g} , and another set of two orbitals, d_{z^2} and $d_{x^2-y^2}$, equivalent to each other but different from the previous set, labeled e_g . The e_g orbitals, which point directly toward the

ligands, are higher in energy than the t_{2g} orbitals, which point between the ligands (Fig. 2a-2). The amount of splitting between e_g and t_{2g} orbitals is generally denoted by Δ or $10 Dq$. The magnitude of Δ obviously depends on the central ion and ligands involved and, according to the CFT, it may be calculated using an electrostatic model. Using an analogous line of reasoning, the splitting patterns of the d orbitals can be obtained for the most important geometries of complexes (Fig. 2a-3).

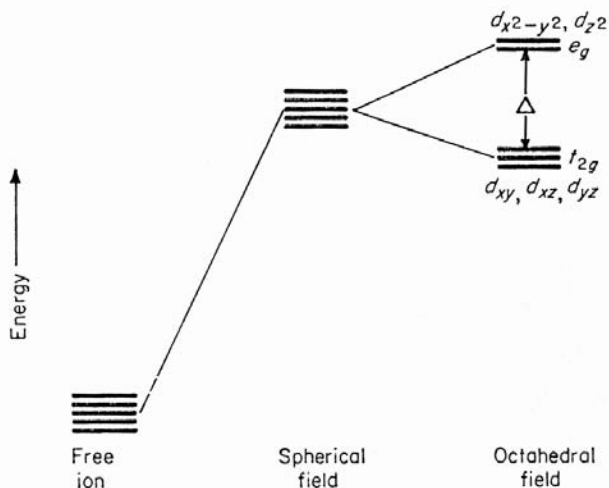


Fig. 2a-2. Splitting of the five d orbitals of a central metal ion in an octahedral field.

Now, let us consider a metal ion with n d -electrons. Owing to the inter-electronic repulsions, the electrons are spread out in the five d orbitals so as to give the maximum number of unpaired spins (rule of maximum multiplicity, or Hund's rule). When the metal ion is introduced into an octahedral environment, the d orbitals split in the manner described above and there will now be a tendency for the electrons to fill the lowest orbitals, t_{2g} , before beginning to go into the upper orbitals, e_g . For a d^1 ion, the single electron will thus occupy one of the t_{2g} orbitals, and the complex can be said to have a t_{2g}^1 configuration. Similarly, for d^2 and d^3 ions, each electron will go into a different t_{2g} orbital and the electron spins will remain uncoupled, as required by Hund's rule. Therefore, the complexes of these ions have a t_{2g}^2 and t_{2g}^3 configuration, respectively. For a d^4 ion, a new and interesting situation arises, since the complex may choose between the following possibilities:

(i) *Low-spin configuration.* All the four electrons go into the three t_{2g} orbitals (t_{2g}^4 configuration); in such a case, two electrons must be coupled in the same

orbital and this requires a certain amount of energy (P) in order to win the interelectronic repulsion.

(ii) *High-spin configuration.* All the four electrons remain unpaired, but one of them must then be promoted to the e_g orbitals ($t_{2g}^3 e_g^1$ configuration); this requires expenditure of the energy Δ .

Of course, the *ground state* of a complex will be represented by the low-spin configuration when $\Delta > P$ (*strong-field* case), and by the high-spin configuration when $\Delta < P$ (*weak-field* case). For complexes containing the same metal ion, P is nearly constant, while Δ strongly depends on the nature of the ligands. Therefore, a metal ion may give high-spin complexes with some ligands and low-spin complexes with other ligands. Octahedral complexes containing more than 4 d -electrons may be treated by the procedure outlined above, and complexes of symmetry other than the octahedral one may be treated by similar procedures.

Besides explaining the magnetic properties of complexes, the CFT enables us to predict, or at least to understand, a number of thermodynamic, kinetic, structural, and spectroscopic features of complexes [6101, 9501].

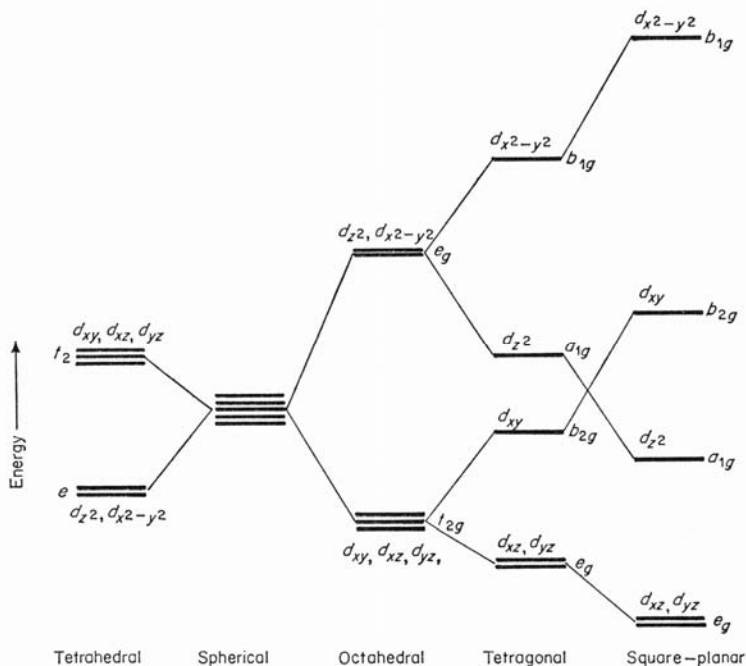


Fig. 2a-3. Splitting of the five d orbitals of a central metal ion in complexes of various symmetry.

2a-2 Ligand Field Theory

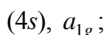
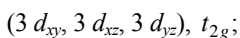
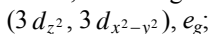
A number of experimental data (electron spin resonance, nuclear magnetic resonance, and nuclear quadrupole resonance spectra, intensities of $d-d$ transitions, nephelauxetic effect, antiferromagnetic coupling, etc.) prove that an appreciable degree of covalency does exist in metal complexes. Therefore, the pure electrostatic CFT model must be considered as a rough approximation of the electronic structure of complexes. A more real approach to this topic must take account of the existence of metal-ligand orbital overlap.

The theory which preserves all the conceptual and computational advantages of the simple CFT and which includes the possibility of accounting for the effects of covalent bonding is called ligand field theory (LFT) [6601, 9901, 0301]. According to this theory, the calculation of the energy level diagrams proceeds in the same manner as in CFT, except that one takes into account that the inter-electronic repulsion and spin-orbit coupling parameters are noticeably reduced when going from free to complexed metal ions, because of the delocalization of the "metal" electrons. In doing this, one either estimates such parameters from experimental observations or assumes that they have values reasonably smaller than in the free ion. Because of its utility, the ligand field theory has enjoyed a wide application by chemists interested in the spectroscopy of metal complexes.

2a-3 Molecular Orbital Theory

In this theory, the molecular orbitals for metal complexes are usually constructed as linear combinations of central metal and ligand orbitals [6401, 6402, 9901, 0301]. In doing this, group-theoretical procedures are usefully employed. Before combining the metal orbitals with the ligand orbitals, one must first consider combinations of the ligand orbitals to obtain sets of composite ligand orbitals (*symmetry orbitals*). The symmetry orbitals of the ligands are then combined with metal orbitals of the same symmetry to produce a set of molecular orbitals into which the electrons are added. The method will now be illustrated for an ML_6 octahedral complex, where M is a first-row transition metal and L is a ligand which possesses both σ and π orbitals. The coordinate system that is convenient for the construction of the MO's is shown in Fig. 2a-4.

(i) *Metal orbitals*. There are nine valence shell orbitals of the metal ion to be considered, that is, the $3d$, $4s$, and $4p$ orbitals. In the O_h point group they may be classified, according to symmetry, as follows:



$(4 p_x, 4 p_y, 4 p_z), t_{1u}$.

The e_g and a_{1g} orbitals are suitable only for σ bonding, the t_{2g} orbitals are suitable only for π bonding, and the t_{1u} orbitals may give both σ and π bonding.

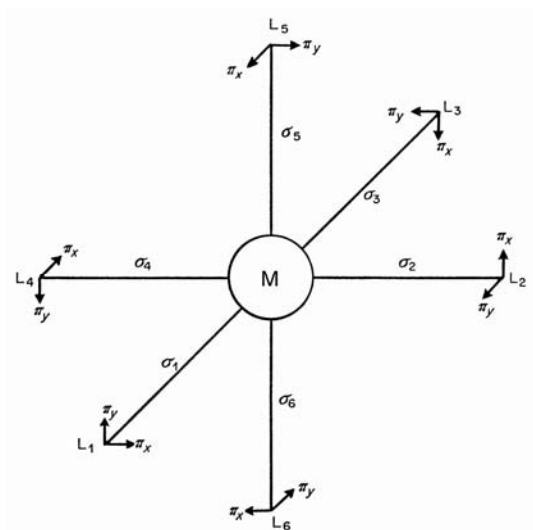


Fig. 2a-4. Coordinate system for σ and π bonding in an octahedral complex.

(ii) *Ligand orbitals.* The individual ligand σ orbitals are combined into six symmetry orbitals. Each one of these is constructed so as to overlap effectively with a particular one of the six metal orbitals which are suitable for σ bonding. This is done by choosing the linear combinations of ligand σ orbitals which have the same symmetry properties as the various metal σ orbitals. (For example, the linear combination of ligand σ orbitals which goes with the $4p_x$ metal orbital has a plus sign in the $+x$ direction and a minus sign in the $-x$ direction. This is the combination $\sigma_1-\sigma_3$.) Similarly, the twelve individual ligand π orbitals (Fig. 2a-4) are combined into twelve symmetry orbitals; six of them will have appropriate symmetry to match the six metal π orbitals, whereas the other six have no metal orbital counterparts and therefore, they will be *non-bonding* with respect to the metal complex. All the σ and π metal and ligand orbitals are shown in Table 2a.

Table 2a Symmetry Classification of Orbitals for Octahedral Complexes

Symmetry representations	Metal orbitals	Ligand orbital combinations	
		σ	π
a_{1g}	$4s$	$\frac{1}{\sqrt{6}}(\sigma_1 + \sigma_2 + \sigma_3 + \sigma_4 + \sigma_5 + \sigma_6)$	
e_g	$3d_{z^2}$	$\frac{1}{2\sqrt{3}}(2\sigma_5 + 2\sigma_6 - \sigma_1 - \sigma_2 - \sigma_3 - \sigma_4)$	
	$3d_{x^2-y^2}$	$\frac{1}{2}(\sigma_1 - \sigma_2 + \sigma_3 - \sigma_4)$	
t_{1u}	$4p_x$	$\frac{1}{\sqrt{2}}(\sigma_1 - \sigma_3)$	$\frac{1}{2}(\pi_{2y} + \pi_{5x} - \pi_{4x} - \pi_{6y})$
	$4p_y$	$\frac{1}{\sqrt{2}}(\sigma_2 - \sigma_4)$	$\frac{1}{2}(\pi_{1x} + \pi_{5y} - \pi_{3y} - \pi_{6x})$
	$4p_z$	$\frac{1}{\sqrt{2}}(\sigma_5 - \sigma_6)$	$\frac{1}{2}(\pi_{1y} + \pi_{2x} - \pi_{3x} - \pi_{4y})$
t_{2g}	$3d_{xy}$		$\frac{1}{2}(\pi_{1x} + \pi_{2y} + \pi_{3y} + \pi_{4x})$
	$3d_{xz}$		$\frac{1}{2}(\pi_{1y} + \pi_{5x} + \pi_{3x} + \pi_{6y})$
	$3d_{yz}$		$\frac{1}{2}(\pi_{2x} + \pi_{5y} + \pi_{4y} + \pi_{6x})$
t_{2u}			$\frac{1}{2}(\pi_{2y} - \pi_{5x} - \pi_{4x} + \pi_{6y})$
			$\frac{1}{2}(\pi_{1x} - \pi_{5y} - \pi_{3y} + \pi_{6x})$
			$\frac{1}{2}(\pi_{1y} - \pi_{2x} - \pi_{3x} + \pi_{4y})$
t_{1g}			$\frac{1}{2}(\pi_{1y} - \pi_{5x} + \pi_{3x} - \pi_{6y})$
			$\frac{1}{2}(\pi_{2x} - \pi_{5y} + \pi_{4y} - \pi_{6x})$
			$\frac{1}{2}(\pi_{1x} - \pi_{2y} + \pi_{3y} - \pi_{4x})$